STUDIES ON A 170 GHz MEGAWATT CLASS CW GYROTRON OPERATING IN THE $TE_{28.12}$ MODE

A DISSERTATION

Submitted in partial fulfillment of the requirements for the award of the degree

of

MASTER OF TECHNOLOGY

in

ELECTRONICS AND COMMUNICATION ENGINEERING

(With Specialization in RF and Microwave Engineering)

By

RAVI KUMAR DHAKAD

DEPARTMENT OF ELECTRONICS AND COMMUNICATION ENGINEERING
INDIAN INSTITUTE OF TECHNOLOGY ROORKEE
ROORKEE-247 667 (INDIA)

JUNE, 2014

CANDIDATE'S DECLARATION

I hereby declare that the work being presented in the dissertation entitled, "***STUDIES ON A 170 GHz MEGAWATT CLASS CW GYROTRON OPERATING IN THE*** $TE_{28,12}$ ***MODE***" in partial fulfillment of the requirements for the award of the degree of ***Master of Technology*** in ***RF & Microwave Engineering***, submitted in the Department of Electronics and Communication Engineering, Indian Institute of Technology Roorkee (India), is an authentic record of my own work carried out under the guidance of Dr. M.V. Kartikeyan, Professor & Head, Department of Electronics & Communication Engineering, Indian Institute of Technology Roorkee.

The matter presented in the dissertation report has not been submitted for the award of any other degree elsewhere.

Date : 29/06/14
Place : IIT Roorkee

Ravi

(Ravi Kumar Dhakad)

CERTIFICATE

This is to certify that the above statement made by the candidate is correct to the best of my knowledge.

Date :
Place : IIT Roorkee

Dr. M.V. Kartikeyan
Professor
E&CE Department
IIT Roorkee

ACKNOWLEDGEMENTS

I would like to express my gratefulness to all who contributed ideas, encouragement and support. I would like to thank, firstly God for giving me grace and wisdom.

I would like to convey my deep sense of gratitude to my supervisor, **Prof. M. V. Kartikeyan**, Head of the Department of Electronics and Communication Engineering, Indian Institute of Technology Roorkee. His continuous support and motivation at every stage of my research encouraged me to give my best efforts. His vast experience on Millimeter, Sub-millimeter and Tera-Hertz wave sources design helped me to resolve practical issues and design optimized systems. Apart from knowledgeable guide he is a person with humble and kind heart. He has always encouraged me for quality research work with innovation and his moral supports.

It is pleasure to thank, **Prof. S.N. Sinha**, **Prof. D. Singh**, **Dr. N.P. Pathak**, **Dr. A. Patnaik** and **Dr. R. Panigrahi**, for their efforts to build my base of RF and Microwave engineering and expand my horizon of knowledge during entire stay in IIT Roorkee.

I would also like to thank **Mr. Arjun Kumar**, **Mr. Jagannath Malik**, **Mr. Kumar Goodwill**, **Mr. Gaurav Singh Baghel**, **Mr. Sukwinder Singh** and **Mr. Himanshu Maurya** with whom I spent most of time during last year. Their valuable support and time to time guidance in technical issues, which was instrumental in making this dissertation work a success. Finally, I would also like to thank all my friends, especially **Ms. Veenu Kamra**, **Ms. Alka**, **Mr. Pranab Kumar Thander** and **Mr. G. G. Krishnamurthy**, for their support and informative discussions.

I specially thank to **Prof. M. Thumm**, Professor, Karlsruhe Institute of Technology, Germany for valuable guidance and review my research publications. I feel

proud to be research member of his group.

I thank **Dr. Jeff Neilson**, Calabazas Creek Research (CCR) for his kind cooperation in carrying out the Launcher design.

Above all, I thank my parents and family members for their never losing trust and confidence on me, even in my tough time and become source of inspiration.

(Ravi Kumar Dhakad)

ABSTRACT

In this work, a conceptual design of 170 GHz Megawatt class Continuous Wave Gyrotron is present. The working mode is $TE_{28,12}$. A diode type Magnetron Injection Gun (MIG) is designed and optimized using Gyrotron Design Suit (GDS) V3 2014 and ESRAY codes. This gyrotron is designed with conventional cavity which includes interaction section with weak input and output taper sections. At place of interaction region super-conducing magnets are used to provide necessary magnetic field 6.725 T for magnetic guidance system. Output system of gyrotron is designed that consists of non-linear taper followed by Quasi-optical launcher and RF window. The softwares used to provide the design of different parts are GDS V3, Gyrotron Cavity Interaction Calculations, Launcher Optimization Tool (LOT) for quasi-optical launcher design and MATLAB for Mirror Synthesis.

Phase Retrieval Algorithm implemented and merged with GDS V3 for conventional Gyrotron and for different planes phase reconstruction has been done. The Iterative Phase Retrieval Algorithm for Gyrotrons employ a numerical solution which determines the phase of the RF wave from the measured intensity profile. Phase reconstruction is achieved by Iterative or Error reduction method in this case. The Phase reconstruction provide profile designing of internal mode converter reflectors and matching optical unit (MOU) for Gyrotrons. The MOU with two mirror system is designed to correct the beam parameters like astigmatism and ellipticity. The correct beam contains almost ideal gaussian content, as more than 99 % pure $HE_{1,1}$ mode is required for optimum performance for electron cyclotron resonance heating (ECRH) transmission system or at plasma end.

Contents

List of Figures

List of Tables

Glossary Items

ECM	Electron Cyclotron Maser
ω	Wave angular frequency
Ω_c	Electron cyclotron frequency
v_z	Translation electron drift velocity
k_z	Axial wave number
γ_{rel}	Relativistic factor
E	Electric field
B	Magnetic Field
P	Momentum of electron
U_{cath}	Cathode voltage
r_L	Larmor Radius
I_{start}	Starting Current
Z_0	Characteristic Impedance
P_{out}	Output Power
α	Velocity ratio
R_c	Cathode radius
R_e	Emitter radius
I_b	Beam Current
b	Magnetic compression ratio
L_c	Quasi optical cut length
tan δ	Loss tangent of material
U_b	Beam voltage
Q_D	Diffracting Quality factor

V_D	Voltage Dipression
I_L	Limiting Current
Self-C	Single-mode self consistence calculation
η	Efficiency of gyrotron
MIG	Magnetron Injection Gun
GDS V3	Gyrotron Design Suite Version 3
NLT	Non-Linear Taper
QOL	Quasi-Optical Launcher
MOU	Matching Optical Unit
Δz_o	Astigmatism
ζ	Ellipticity

Chapter 1

Introduction

Gyrotrons are the fast wave (phase velocity is higher than the light velocity) devices which are capable to delivered kilo-watts to Mega-watts of power at millimeter/sub-millimeter/tera-hertz wave frequencies. From their conception in the late fifties until their successful development for various applications, gyrotrons have come a long way technologically and made an irreversible impact on both users and developers. Gyrotron technology has significantly advanced from single frequency low power to multi-frequency high power during this time towards meeting the goals for reliable and efficient source of high power in millimeter and sub millimeter wavelength range.

1.1 General Introduction

The gyrotron is a millimeter/sub-millimeter beam source that generate the high power coherent radiation. It consist a magnetron injection gun (MIG). The MIG produces an annular electron beam, which goes into a cavity resonator. The cavity resonator is in the presence of an axial magnetic field. The axial magnetic field is created by a special super–conducting magnets. In the open cavity, the RF field comes in the interaction with electrons in the beam which are in cyclotron motion, due to this interaction kinetic energy of moving electron is converted in RF energy.

Now extracting this RF output can be achieved by two methods:

1. Axial output coupling RF power in TE_{mn} mode is taken by axial vacuum window.

2. A quasi-optical launcher (QOL) or mode convertor is used for conversion of TE_{mn} mode to gaussian mode so power will flow radially, then radial power transmitted by a radial vacuum window.

Gyrotron systems have proven useful where conventional microwave sources have not been able to fulfil the requirements of some specific applications. This is demonstrated by the number of applications in which they can be found. There are many applications of gyrotron such as [1]:

- Plasma heating and plasma diagnosis.
- Satellite communication.
- Radar ranging and imaging.
- Sub-millimeter wave and THz spectroscopy.
- Materials sintering and processing.

1.2 High Power Continuous Wave Gyrotrons

High frequency high power gyrotrons are mainly developed for microwave heating and current drives in plasmas for thermonuclear fusion research. Electron cyclotron resonance heating (ECRH) and electron cyclotron resonance current drive (ECCD) have proven to be important tools for plasma formation devices especially for stellarator and TOKAMAKS, as it provides both net current-free plasma startup from the neutral gas and efficient heating of the plasma [2].

For the international thermonuclear experimental reactor (ITER) desired power for 1800 seconds pulse is 2 MW from a single gyrotron. The maximum pulse length

is achieved by 140 GHz, megawatt-class gyrotron is 60 minutes with 0.92 MW output power, 44% efficiency and 97.5 % Gaussian mode content. This gyrotron build under the collaboration of CPI and European KIT-CRPP-CEA-TED. It is employing synthetic diamond output window and single-stage depressed collector [3].

1.3 Plasma Heating Techniques in nuclear Fusion Reactors

The research going on the thermonuclear fusion reactor to fulfil the energy need in the future. The nuclear fusion is the cleanest and safest way to generate the power. The process of nuclear fusion is two low nuclear mass positively charged nuclei collide to each other at high temperature. The lighter nucleus fuse to heavier nucleus. In doing, this process they release a large amount of energy. Fusion power is a most researching area plasma physics. To fuse the Deuterium-Tritium atoms, the required temperature is in the range of 100 - 150$\times 10^6$ °C.

1.3.1 Ohmic Heating/Current Drive

Plasma behaves as an electric conductor because it is nothing but a ionized gas. It can be heated by inducing current through it. In a plasma torus, there are electromagnetic winding outside. When we apply the current on these windings, the induced current developed in the plasma. We can understand this mechanism by taking an example of a transformer. The winding is primary coil and plasma is a secondary coil. This is instinctively a pulsed process because there is a limit to the current through the primary (there are also other limitations on long pulses). So, this type of heating called ohmic or resistive heating.

1.3.2 Neutral Beam Heating

In this type of heating, a high - energy beam of neutral atoms injects. Generally these are isotopes of hydrogen atom such as deuterium and tritium. These highly energized atoms transfer their energy to the plasma. The transfer of this energy gives the increment in the temperature.

1.3.3 Radio-Frequency Heating

In this type of heating radio waves inject into the plasma at a fixed frequency. At this frequency the particles in plasma resonate with a fixed rotation, and these wave particles transfer their energy to plasma particles. These plasma particles have different resonance frequencies. Therefore the heating can be applied selectively to a defined group of particles in a defined location in the plasma, by injecting radiation at just the right frequency. This is known as Ion-Cyclotron Resonance Heating (ICRH).

1.4 Motivation and Scope

The generation of power is getting very crucial day by day, to overcome the problem of generation of power we need to decide an alternative of classical power generation methods. The nuclear fusion promises these as it is the most safest and cleanest method and can generate huge amount of power. so, the most important use of gyrotrons are heating of plasmas in nuclear fusion experiments reactors. Another applications are high temperature processing and sintering of materials. The designing of gyrotrons for nuclear fusion experiments extends from long pulse to real CW regime with the highest power while maintaining the higher efficiency.

Presently ITER is the largest nuclear fusion project is under developing under the collaboration of seven countries, European Union (EU), Unites States of America (USA), India, People's Republic of China, Russia, Japan, South Korea. The operat-

ing frequency varies from 30 to 170 GHz of gyrotrons in the ITER [4]. Presently, the goal of researchers is to achieve the maximum output power, maximum efficiency and maximum pulse duration. Along with this project, another project which is named as steady state super conducting TOKAMAK (SST-1) is under the fabrication and designing at the Institute for Plasma Research (IPR) Gandhinagar, India with relatively low magnetic field and power generation [5].

The goal of this work is to designing of CW operation of a 170 GHz gyrotron with an output power of the level of MW for plasma heating application like ITER. And designing the complete output system along with mirror synthesis and checking the working of Iterative Phase Retrieval Algorithm (IPRA).

1.5 Related Literature Review

Gyrotron fulfil the requirements of the applications in whereas the conventional microwave sources cannot. Substantial work on gyrotrons has been done in the development of gyrotrons for plasma diagnostics in thermonuclear fusion experiments, material processing, technological applications and medical applications [6]- [9].

This section explains the details about the various development programs of gyrotrons operating at the frequency of 170 GHz around the world. The practical implementation of the concept of electron cyclotron resonance maser explored in late 1950's and later than in mid sixties. Russia starts to develop the earliest version of the gyrotrons. From that point the gyrotron technology starts to move fast and now the latest versions of gyrotrons are capable to fulfil the requirements of the applications. Gyrotrons require super conducting magnets to control the beam parameters. At the end of ninetieth century the super conducting magnets are not available, which stopped the development of high power gyrotrons. The ITER project had begun in 1985. In this project 24 gyrotrons are required and for each

gyrotron approximately 2 MW power required to deliver of 170 GHz gyrotron. This step attracted scientist for designing high power 170 GHz gyrotron [10].

Mainly three teams of different countries have worked on 170 GHz Gyrotron.

- Plasma Heating Laboratory, Japan Atomic Energy Agency (JAEA) in coloration with Toshiba Electron Tubes & Devices Co.,Ltd., Japan.
- The GYCOM collaborates with the Institute of Applied Physics(IAP), Russian Academy of Sciences, Nizhny Novgorod, Russia.
- Karlsruhe Institute of Technology, Karlsruhe, Germany.

In the starting of the twentieth century JAEA started a program to develop 1 MW, 170 GHz, continuous wave (CW) gyrotron for ITER. They used conventional cavity, working mode $TE_{31,8}$ with quality factor (Q) was 1503. The distribution of the power is converted into a Gaussian beam from the in-built mode-converter. The Gaussian output power is taken out by edge cooled diamond window. The beam voltage and beam current was 71.2 kV and 20-30 A respectively. For the 100 seconds and 9.2 seconds they achieve 0.5 MW and 900 KW respectively. They achieve these results in 2004. To achieve the more better results they modified the design. They replace their conventional gun with the triode type magnetron injection gun, which provide more flexibility in the pitch factor. And at the end of 2009 they achieve 800 KW, CW RF output power with the 35 % efficiency. The beam voltage and current were 72 kV and 29.5 A. The group is also working on the designing of dual frequency regime gyrotrons for the frequencies 170 GHz and 137 GHz with $TE_{33,11}$ and $TE_{25,9}$ modes respectively. The most common applications of 170 GHz is ECRH and 137 GHz is ECCD in TOKAMAKs. In 2011 by applying 40-70 A beam current they achieved 1-1.2 MW power at the both frequencies. [11]- [20].

The collaborative group GYCOM/IAP designed 170 GHz gyrotron in 2000. At the starting they used boron Nitride (BN) window which provides low transmission

of the output RF beam. Then they collaborate with the Karlsruhe Institute of Technology (KIT), Chemical Vapor Deposition (CVD) Diamond window was installed. They achieved 32 % with 800 KW output power. And after using single stage depressed collector (SDC) the achieved efficiency was 52 %. They built this gyrotron at $TE_{28,12}$ and $TE_{25,10}$ modes. The both modes are best to deliver CW output power. The beam voltage and beam current ranges in this gyrotron were 70-100 KV and 40-50 A [21]- [28].

Besides of the others, Karlsruhe Institute of Technology, Karlsruhe, developed Coaxial cavity gyrotron. The output power of this gyrotron is equal to 2 MW and operating at the $TE_{34,19}$. The applied beam voltage and beam current are 90 KV and 75 A respectively. The Magnetic field at interaction was 6.87 T and the beam velocity ratio is 1.3. Along with this gyrotron they are also developed 140 GHz and 170 GHz conventional cavity gyrotron [29]- [35]. All previous efforts for development of 170 GHz gyrotrons are presented in Table 1.1.
The un-availability of super-conducting magnets limits the output power. At the beginning stage a 6 T can produce by normal magnets, but due to availability of super-conducting magnets the magnetic field can be achieved up to 7 T. The CVD diamond window and single stage depressed collector increase the efficiency of gyrotrons [36]- [37].

Table 1.1: Development of 170 GHz Gyrotrons by different companies and Institutions under various collaborations

Organization	Mode	Power (MW)	Efficiency (%)	Beam Voltage (KV)	Beam Current(A)
JAEA,TOSHIBA	$TE_{31,8}$,$TE_{33,11}$	1-1.2	35	70 - 90	40-60 A
GYCOM-N	$TE_{25,10}$,$TE_{28,12}$	1	32	70-100	40 - 70 A
KIT, Karlsruhe	$TE_{34,19}$(Coax.)	2	50	90	75 A

1.6 Problem Statement

- Checking the feasibility of 170 GHz Megawatt class Continuous wave conventional cavity gyrotron.
- The following tasks are investigated, performed and designed:
  - Mode Selection.
  - Conventional cavity design.
  - MIG and magnetic guidance system design.
  - Studies on RF - behavior.
  - A Non - linear taper design.
  - Advanced dimpled - wall quasi - optical launcher.
  - RF window.
  - Phase retrieval.
  - Mirror synthesis.

1.7 Organization of the Thesis

There are five chapters compiled in this dissertation including the present chapter.

- ***Chapter one*** gives a brief introduction of fundamental harmonic gyrotron and nuclear fusion techniques, along with the motivation and scope and related literature review of 170 GHz, Megawatt class fundamental harmonic gyrotron. The literature review gives the details of various gyrotron development projects goes under the ITER project.
- ***Chapter two*** presents the related gyrotron theory which includes the basic principle of gyrotrons, design feasibility, starting currents, beam - wave interaction, RF behavior. The theory for the designing various parts are also given in this chapter. Initial design of each component has been carried out using

GDS V3 2014 (Gyrotron Design Suit Version 3). This chapter also includes brief introduction about GDS package which contains the new features like phase retrieval and mirror synthesis.

- ***Chapter three*** deals with the design studies of the application specific 170 GHz, MW, CW gyrotron operating at fundamental harmonic. The results of all the procedures have been given with detailed analysis. It starts from design feasibility (mode selection), cavity design, RF behavior, MIG and magnetic guidance system design. This chapter also includes the output system which contains a non - linear taper, a quasi - optical launcher and RF window.

- ***Chapter four*** includes the Iterative Phase Retrieval Algorithm (IPRA) to get the phase information on different planes after the launcher and after the window. The chapter also includes the designing of mirrors using a latest mirror synthesis approach to correct the beam purity. So that, it can couple better to the corrugated waveguide.

- ***Chapter five*** concludes the thesis work with the concluding remarks and outline direction for future scope.

Chapter 2

Gyrotron Theory

In this chapter, the theories and principles of gyrotron is given. This chapter presents useful gyrotron equations, includes the interaction of RF field with the electron beam and the conversation of the kinetic energy to the RF energy in the cavity. The detailed description of all the components are are also presented in this chapter.

2.1 Principle of Operation

The arrangement of a simple gyrotron is given in Fig. 2.1. Here, a magnetron based electron injection gun is situated below in the figure. When voltage is applied at emitter it generates electric field. This electric field consists perpendicular and parallel components with respect to the lines of the magnetic field produced by a solenoid. Now when electrons emitted from the cathode it has orbital and axial velocity components. Then, electrons will move forward to interaction region in the increasing magnetic field, the electrons flow undergoes the adiabatic compression so electron orbital momentum increases. Now In the uniform magnetic field region, the electrons interact with the mode of the cavity and transform a part of their kinetic energy into RF energy. Then, the beam exits from the axially open cavity settles on the collector with decreasing magnetic field. The RF output power in the TE_{mn}

mode is coupled through the axial output vacuum window.

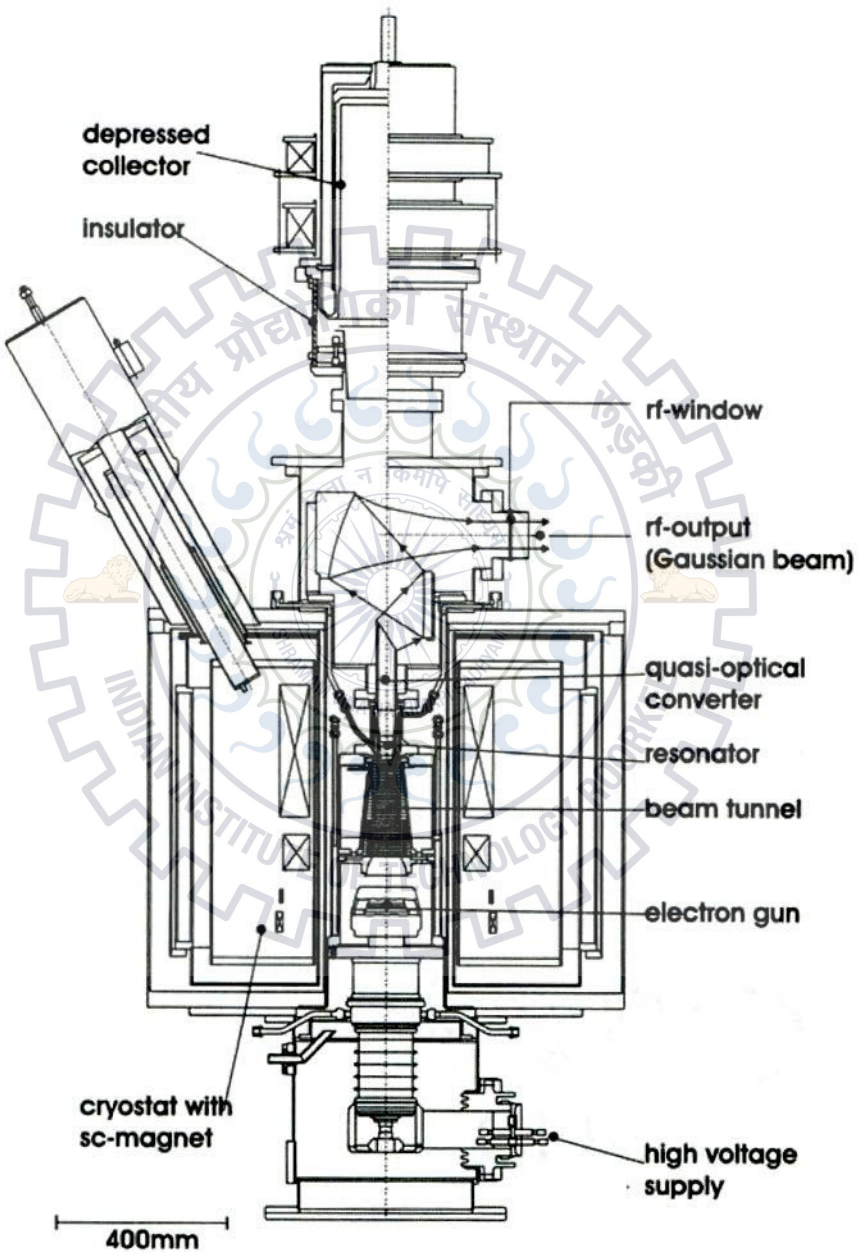

Figure 2.1: Schematic of a higher order volume mode gyrotron [1].

Classical microwave tubes require interaction structures smaller than a wavelength due to electron coherent radiation involved. Gyrotrons however, operate on the prin-

ciple of cyclotron resonance. In these kind of devices, the electrons can resonantly interact with fast waves, which can propagate even in free space. Therefore, the interaction space in gyrotrons can be much larger than in classical microwave tubes operating at the same wavelength. In such circuits the phase velocity v_{ph} of the EM wave is higher than velocity of light (c) [38].

In fast wave devices electron undergoes in oscillation transverse to the direction motion of beam by the action of external field, so they radiate. This is the condition of coherent radiation, which is obtained when mechanism of bunching exists to create electron density variation of size compare with wavelength of the electromagnetic wave. To obtain this mechanism, a resonance condition is satisfied between the periodical movement of the electron and EM wave in the interaction section.

$$\omega - k_z v_z \cong s\Omega, s = 1, 2, ...(k_z v_z = Doppler'sterm) \tag{2.1}$$

Here ω is angular frequency of wave, k_z is axial wave number, v_z is electron velocity, Ω is an effective frequency, which is related with oscillated motion of the electrons, and s denotes harmonic number. In ECM, EM energy is radiated by electrons which are gyrated in an external longitudinal magnetic field. The effective frequency corresponding to the electron cyclotron frequency is given as

$$\Omega_c = \Omega_{co}/\gamma_{rel} \quad where \quad \Omega_{co} = eB_o/m_o \quad and \quad \gamma_{rel} = [1 - (v/c)^2]^{-1/2} \tag{2.2}$$

here γ is the relativistic mass factor. A group of relativistic electrons is gyrated in high magnetic field will radiate coherently.

The transverse velocity component of electrons spiraling in the existence of applied magnetic field interact with the transverse electric (TE) modes of cavity. An electron with a transverse velocity component which is opposite in direction of the electric field gains some energy (in this case γ increase), then its resonance frequency decrease and the electron begins to fall behind the phase of the oscillatory E field. In another case An electron with a transverse velocity component which is in same direction as the electric field so it loses some energy (γ decrease), then its resonance frequency increase and the electron begins to takeover the phase of the E field. After

certain orbits electrons which were initially distribute uniformly with respect to the phase of the electric field become tightly bunched in phase [39]. Energy is extracted from the tightly bunched electrons only when the frequency of the oscillatory electric field is higher than the cyclotron resonance frequency, then electron bunches are situated in the decelerating phase of the electric field.

In cylindrical cavity gyrotrons with radius R_0 the operating mode is close to cut-off ($v_{ph} = \omega/k_z \gg c$) and to keep the electron bunches in the retarding phase the frequency mismatch ω-sΩ_c is less but positive value. The Doppler term $k_z v_z$ is of the order of the gain width and is small as compared to radiation frequency. Harmonic operation decreases the requirement of magnetic field at a given frequency by factor s. Dispersion diagram for fundamental harmonic is shown in Fig. 2.2.

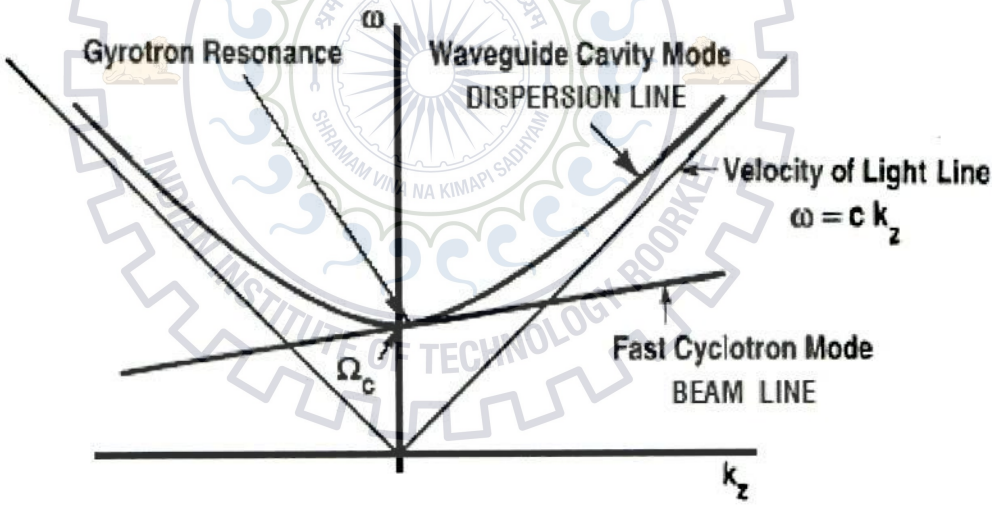

Figure 2.2: Dispersion diagram of gyrotron for fundamental Resonance [40].

2.2 Theory of Gyrotrons

This section presents the practical considerations for gyrotron design, keeping in mind the design constraints. In addition, the theory behind the starting current calculations and beam wave interaction is also discussed.

2.2.1 Design Feasibility - Mode Selection

The designing of a particular gyrotron always implicate number of mutually inconsistent design aims and duress. The general design constraints for high power gyrotrons are shown in Table 2.1. The values of all these constraints are calculated for all the competing modes of the particular gyrotron. Only one mode is selects for the designing of that gyrotron.

Table 2.1: Gyrotron design constraints.

Paramter	value
Peak Ohmic wall Loading (p_{wall})	$< 2.0\ kW/cm^2$
Voltage Depression ($\Delta V/V$)	< 0.1
Ratio of beam current to limiting current (I_b/I_L)	< 0.5
Magnetic Compression ($b_{comp} = B_{cav}/B_{gun}$)	< 50
Electric Field at the Emitter(E_e)	< 7 kV/mm
Emitter mean radius (R_e)	< 50 mm
Cathode Current Density (j_e)	$< 4\ A/cm^2$
Fresnel Parameter (C_F)	≈ 1.0

1. Wall Loading

High power gyrotrons suffers from the wall losses, a cooling system used to cool the walls of gyrotrons. For the cooling system it is important to calculate the wall losses. This depends into two types of losses, one is local wall loading and other is total wall loses. The definition is the ratio of integrating RF power flow in the walls of cavity divided by its surface area [1]. Wall losses can be calculated by the equation:

$$\left(\frac{dP}{dA}\right)_{max} \approx \sqrt{\frac{8}{\pi}} \sqrt{\frac{1}{\pi Z_0 \sigma}} \frac{PQ}{L\lambda^{1.5}} \frac{1}{x_{mp}^2 - m^2} \tag{2.3}$$

where L is length of effective Gaussian field profile, Q is the ohmic quality factor of resonator cavity and Z_0 is free space impedance whose value is equal to 377 Ω.

2. Voltage Depression

Voltage Depression (V_D) is the reduction of the potential within the beam tube due to the beam space charge. V_D for a hollow beam of radius R_b is equal to [39]:

$$\Delta V_D \approx 60\Omega \cdot \frac{I_b}{\beta_z} \cdot \ln\left(\frac{R_0}{R_b}\right) \tag{2.4}$$

where R_b is the beam radius, and β_z is the axial velocity ratio. The upper limit for voltage depression is roughly estimated to be around 10% of the applied accelerating voltage above this value instabilities may occur. Effect of this depression can be reduced by increasing the beam voltage.

3. Limiting Current

The limiting current I_L is defined as current for which the voltage depression value is very high so that propagation of electron beam is not possible ($\beta_z \to 0$ and mirroring of the beam occurs). Limiting current must be double then operating current [1]. It is given as:

$$\frac{I_L}{8500A} \approx \frac{I^*}{\ln\left(\frac{R_0}{R_b}\right)} \tag{2.5}$$

$$I^* = \gamma_0 \left[1 - \left(1 - \beta_{z0}^2\right)^{1/3}\right]^{3/2} \tag{2.6}$$

where $\beta_z = [1 - \beta_\perp^2 - 1/\gamma^2]^{1/2}$. Here γ_0 and β_{z0} represent the values in the absence of voltage depression.

4. Fresnel Parameter

This parameter is introduced by a Russian researchers called the Fresnel parameter (C_F) which describe how a specific mode will oscillates [1]. It is defined as

$$C_F = \frac{L^2}{8R_0\lambda\sqrt{1-\left(\frac{m}{x_{mp}}\right)^2}} \tag{2.7}$$

where L is the effective length of the interaction region. It describes the effective diffraction of a wave at the taper transitions in a resonator. For TE modes near cut–off, $(2\pi/\lambda) \simeq (x_{mp}/R_0)$ which simplifies the expression for the Fresnel parameter as:

$$C_F \cong \frac{\pi}{4} \cdot \frac{\left(\frac{L}{\lambda}\right)^2}{\sqrt{x_{mp}^2 - m^2}} \tag{2.8}$$

Though this modified expression is considered as the original definition for the Fresnel parameter but the relevance of the cavity radius R_0 in C_F as given in eq. 2.7 is much more important. According to Gaponov [41], cavities with $R_0 \geq L$, the Fresnel parameter is rather small $C_F < 1$. This gives an unfixed longitudinal and transverse structure of the RF field. Therefore, it may be interpreted that in the case of operation with higher modes when $R_0 \geq L$, the fixation of the longitudinal and transverse structure of the RF field is difficult [1]. So it is probable that a value of $C_F > 0.5$ is desirable, but $C_F \geq 1$ is not necessary.

2.2.2 Starting Currents

A gyrotron starts oscillation when the starting current I_{start} goes beyond to the minimum acceptable value. The value of I_{start} depends on the beam radius, cavity radius, cavity mode, etc. Starting current separate the desired mode with the other competing modes. Also to couple electron beam effectively starting current calculation is done [1]. This I_{start}, it is the minimum amount of current when $dP_{out}/dt > 0$ in the limit $P_{out} \to 0$:

$$I_{start} = \left(U \frac{d\eta}{dP}\bigg|_{P=0} \right)^{-1} \tag{2.9}$$

gyrotron operation is occurred only when $I > I_{start}$, and $dP_{out}/dI_b > 0$. To initially compute the starting currents of main or operating mode and its competing mode for preliminary assessment, a gaussian field profile is employed.

This starting current calculation is done in a linearized single-mode theory. This is explain below [1].

$$\frac{-1}{I_{start}} = \left(\frac{QZ_0 e}{8\gamma_0 m_e c^2} \right) \left(\frac{\pi}{\lambda} \int_0^L \left| \hat{f}(z) \right|^2 dz \right)^{-1} \cdot \left(\frac{k_{mp} C_{mp} G_{mp}}{\beta_{z0}(s-1)!} \right)^2 \left(\frac{c k_{mp} \gamma_0 \beta_{\perp 0}}{2\Omega_0} \right)^{2(s-1)} \cdot \left(s + \frac{1}{2} \frac{\omega \beta_{\perp 0}^2}{v_{z0}} \frac{\partial}{\partial \Delta_s} \right) \cdot \left| \int_0^L \hat{f}(z) e^{i\Delta_s z} dz \right|^2 . \tag{2.10}$$

where

$$\Delta_s(z) = \frac{\omega}{v_{z0}} \left(1 - \frac{s\Omega_0(z)}{\omega\gamma_0} \right)$$

$$Z_0 = \sqrt{\mu_0/\epsilon_0} \simeq 377\Omega$$

$$k_{mp} = \frac{x_{mp}}{R(z)}$$

$$G_{mp} = J_{m-s}(k_{mp}R_e) \quad \text{for co} - \text{rotating modes}$$

$$= (-1)^s J_{m+s}(k_{mp}R_e) \text{ for counter rotating modes}$$

$$\frac{J^2_{m\pm s}\left(\frac{x_{mn}R_e}{R_o}\right)}{\pi(x^2_{mn}-m^2)J^2_m(x_{mn})} \tag{2.11}$$

If this is too small for a given mode, the starting current will be large and the mode is unlikely to oscillate [39]. If starting current is too high, then rise times of field and current can be comparable and field cannot react fast enough to a change in the current. This becomes a problem in the pulsed mode.

2.2.3 Beam–wave Interaction

The beam - wave interaction is a process in which the electron beam transfers its kinetic energy to the transverse E-field mode in the cavity. The process involves the suspicious design of the cold cavity structure (interaction circuit) and the study of RF - behavior.

Interaction Structure

The design of the cavity structure for gyrotron depends on some parameters such as field features, resonator's eigen frequencies, and quality factor (Q) which are related to the resonance frequency. A reasonable design will lead to eduction of microwave power effectively. In conventional gyrotrons, the cavity consists three different length structure of length L_1, L_2, L_3, first is input taper then it is followed by a uniform mid–section length(L_2) where the interaction occurred then at the last output up-taper comes. A simple resonator structure is given in Fig. 2.3.

The up-taper stops the backward propagations of RF wave. For undesired mode conversion instead of abrupt change the parabolic smoothing is preferred. The interaction of beam - wave occurred in the mid - section. At the center RF - field gives high value. And at later stage the up-taper connects the output waveguide and then mode converters.

Due to Reflections generated in tapers resonant behavior is started a wave is transmitted with high efficiency from cavity. ω and Q are determined by applying

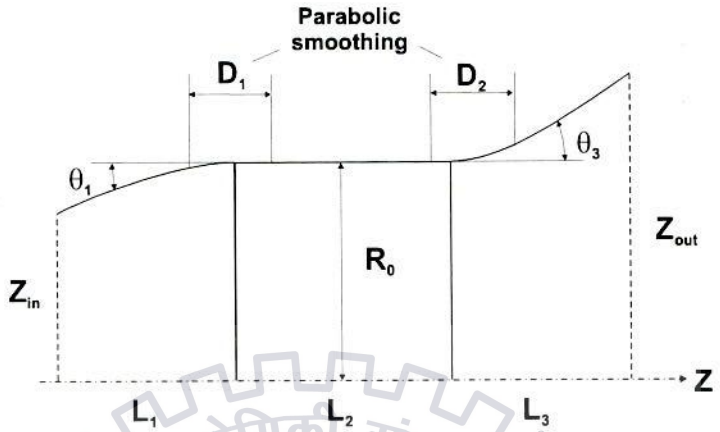

Figure 2.3: Resonator geometry [1].

boundary conditions on resonator output taper [42]. Procedure to determine the eigenmodes in cavity is to solve wave equation. In the cavity geometry by applying radiation boundary conditions we obtain minimum reflections for resonant frequencies of the eigenmodes.

In cold cavity analysis, V_{max} and the output power are related by:

$$QP_{\text{out}} = \omega W = \left(\frac{\omega c_0}{2}\right) V_{\text{max}}^2 \int_{z_{\text{in}}}^{z_{\text{out}}} \left|\hat{f}_{mp}(z)\right|^2 dz. \tag{2.12}$$

where, $\hat{f}_{mp}(z)$ is the field profile normalized to a maximum absolute value 1.

RF–Behavior

To compute the efficiency, output power and energy loss or gain, equation of motion for a single electron must be solved numerically. The equation will be solved for a single electron which is in the impendence of E and H field.

In cold cavity calculations, the adiabatic approximation to equation of electron motion is derived and this equation of motion is solved in the fixed field approximation to compute the efficiency. In self - consistent calculations, the equation of motion is solved simultaneously with the field equations, taking into account the effect of beam

on the cavity field profile and quality factor, as well as frequency pulling [43, 44]. Derivation is given here

$$\vec{u} = \gamma\vec{v}/c \tag{2.13}$$

and

$$P = iu_{\perp}e^{-i(\Lambda+\theta_c)} = u_{\perp 0}\tilde{P} \tag{2.14}$$

where Λ is varied very slow in parts of the gyro phase. The equation of motion for electrons in the field of a TE_{mp} mode can be decreased to

$$u_z \approx \text{constantvalue} \tag{2.15}$$

$$\frac{d\tilde{P}}{dz} + i\frac{\omega}{v_{z0}}\frac{1}{s}\left(\frac{\gamma}{\gamma_0} - 1 + \delta\right)\tilde{P} = i\frac{\omega}{v_{z0}}\frac{\gamma}{\gamma_0}F_{mp}\hat{f}_{mp}(z)\left(\frac{ck_{mp}u_{\perp 0}\tilde{P}^*}{2\Omega_0}\right)^{s-1} \tag{2.16}$$

Here $\hat{f}(z)$ is the normalized field profile, δ is detuning parameter

$$\delta = 1 - \frac{s\Omega_0}{\gamma_0\omega} \tag{2.17}$$

and

$$F_{mp} = \frac{eV_{max}}{2mc^2}\frac{C_{mp}G_{mp}}{u_{\perp 0}}\frac{ck_{mp}}{\omega}\frac{1}{(s-1)!} \tag{2.18}$$

is relate with

$$F_G = \left(\frac{s\beta_{\perp}^2}{2}\right)^{s-2}F_{mp} \tag{2.19}$$

Also

$$C_{mp}G_{mp} = \pm\frac{J_{m\pm s}(k_{mp}R_e)}{J_m(x_{mp})\sqrt{\pi(x_{mp}^2 - m^2)}} \tag{2.20}$$

The output power in TE_{mp} mode is given by the Poynting's theorem. [41]:

$$P_{out} = V_{max}^2 Re\left(\frac{1}{2i\mu_0\omega}\,\hat{f}_{mp}\,\frac{d\hat{f}^*_{mp}}{dz}\right) \tag{2.21}$$

evaluate at the output of resonator and consider

$$\frac{ck_{mp}u_{\perp 0}}{2\Omega_0} \simeq \frac{s\beta_{\perp 0}}{2}$$

In a self-consistent, the field profile should satisfy

$$\frac{d^2F_{mp}\hat{f}}{dz^2} + \left(\frac{\omega^2}{c^2} - k^2_{mp}(z)\right)F_{mp}\hat{f} = -\hat{I}\left(\frac{-ick_{mp}u_{\perp 0}}{\Omega_0}\right)^{s-1}\langle\tilde{P}^s\rangle \tag{2.22}$$

Here

$$\hat{I} = \frac{eZ_0I_b}{2mc^2}\left(\frac{C_{mq}k_{mp}G_{mp}}{(s-1)!}\right)^2\cdot\frac{1}{u_{z0}}$$

where $Z_0 = \sqrt{\frac{\mu_0}{\epsilon_0}}$ and $k_{mp}(z) = \frac{x_{mp}}{R(z)}$, with radiation boundary condition at output.

2.3 Components of Gyrotron

2.3.1 MIG and Magnetic Guidance System

Gyrotrons need a high power, hollow, electron beam with orbital energy and small velocity spreads. The development of powerful magnetron injection gun for gyrotron has play a major role in making these devices powerful coherent radiation sources. MIG generates annular electron beam, this beam electron executes small cyclotron orbit at a frequency at which cyclotron resonance interaction occurred in gyrotron.

For higher frequencies such as greater than 30 GHz, Magnetic field is higher then 1 T is used for operate at fundamental cyclotron resonance. Super–conducting magnetic

coils are generally employed. Magnetic field is given in Tesla at any frequency is related to frequency by$f\ (GHz).\gamma/28$, where f is the operation frequency(GHz) and γ is the relativistic factor. Most magnet consist of one or two main cavity magnet coils and a gun coil for adjusting the magnetic field in the cathode. Magnet coils are used for shaping fields in collector.

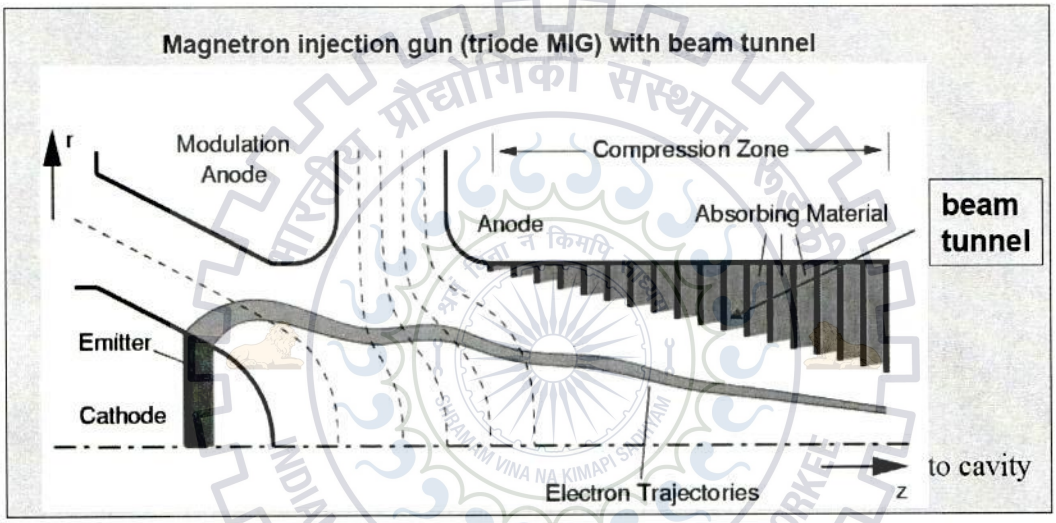

Figure 2.4: Schematic of MIG with the Electron Beam Tunnel [1].

The region started at the MIG and end at entrance of the cavity is called the beam tunnel shown in Fig. 2.4. In this compression region electron beam radius and wall radius decreases from starting to end. The beam tunnel has structure of alternating metal–damping ceramic rings. This has special shape rings which are made by lossy ceramic for suppressing unwanted oscillations and beam instability.

Trade–off and initial design expressions for a Magnetron Injection Gun are given below. The initial design establishes the main gun parameters such as radius of cathode (average), spacing between anode and cathode, emitter current density, E field at cathode, and cathode slant angle to the required beam properties. After that the simulation codes are used for a final optimization of the shape of the electrodes.

- Electron energy U_b and relativistic mass factor:

$$\gamma_0 = 1 + \frac{U_b}{511\,\mathrm{kV}} = \frac{1}{\sqrt{1-\beta_{\perp 0}^2-\beta_{z0}^2}} \tag{2.23}$$

- Beam power $U_0 I_b$, where U_0 is the accelerating voltage and I_b is the total beam current.

- Optimum cyclotron frequency:

$$\omega_c = \frac{eB_0}{m_e\gamma_0}. \tag{2.24}$$

- Larmor radius at interaction:

$$r_{L0} = \frac{v_{\perp 0}}{\omega_c} = 1.705\,\mathrm{mm} \times \frac{\gamma_0\beta_{\perp 0}}{B(\mathrm{T})} \tag{2.25}$$

- Velocity ratio:

$$\alpha = \frac{v_{\perp 0}}{v_{z0}} \tag{2.26}$$

- The radial thickness of the beam at interaction should not exceed $\lambda/8 + 2r_{L0}$.

The other parameters should be chosen to provide the above beam parameters with minimal velocity spread. These include:

- Compression ratio:

$$b = \frac{B_0}{B_c} \tag{2.27}$$

- Emitter Radius:

$$R_c = \sqrt{b}R_e \tag{2.28}$$

and the emitter radius thickness can be estimated from

$$\Delta R_c = \sqrt{b}\Delta R_e. \tag{2.29}$$

- Emitter Length: Simple geometry determines the emitter length l_s from total current

$$I_b = (2\pi R_c l_s)J_c, \tag{2.30}$$

where ϕ_c is the cathode slant angle and J_c is the cathode current density, note that (also)

$$\Delta R_c = l_s \sin \phi_c. \tag{2.31}$$

- Cathode electric field: A first estimate of the required cathode electric field E_c can be obtained from

$$\gamma_0 v_{\perp 0} = \sqrt{b}\gamma_c v_{\perp c} = \frac{\sqrt{b} E_c \cos \phi_c}{B_c}, \tag{2.32}$$

and this requires

$$E_c \cos \phi_c = \frac{B_0 \gamma_0 v_{\perp 0}}{b^{3/2}}. \tag{2.33}$$

- Cathode–anode spacing: The cathode–anode spacing (d) is given by

$$d = R_c \frac{r_{L0} D_F \mu}{\cos \phi_c}, \tag{2.34}$$

where D_F is the cathode–anode spacing factor (select $D_F \geq 2$) and μ is Tsimring cylindricity parameter ($= 1/\sqrt{(r_{g0}/r_{L0})^2 - 1}$ and r_{g0} is the guiding center radius at the RF interaction region).

2.3.2 Interaction Cavity

Interaction cavity for gyrotrons consists a simple cylindrical structure with a input taper at the cavity starting position and output taper at cavity exit as shown in Fig. 2.7. These device operation are effective near cutoff frequency of the operating TE mode in interaction cavity. In cavity, mild tapers are at the starting and end of the cavity for providing required reflections to introduce a standing wave in cavity. The frequency of the $TE_{m,p}$ resonance is set corresponding to the operating frequency, which must satisfy the cyclotron resonance condition. The beam wave interaction has already been discussed in previous section.

One of the major advantage of gyrotrons is that the interaction is relatively insensitive to the beam quality, especially in oscillators [42]. The design trade off that determine the choice of cavity modes are:

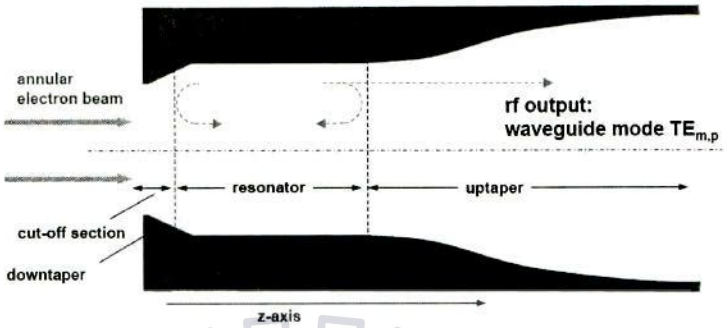

Figure 2.5: Schematic of Interaction Cavity

- Wall loss in the cavity should be ($P_{max} < 2\text{kW}/cm^2$).
- Voltage depression should be less.
- careful mode selection.

All these requirements are met by only higher order modes. The coupling of the operating mode with electron beam is strong when small beam radius in the resonator coincide with inner E field maximum .

2.3.3 Non–Linear Taper (NLT)

Tapered transmission lines (tapers) are used to transfer the output from cavity to oversize waveguide component. The taper is designed in a fashion so that the Z_0 should be match at both the ends. There are two types of taper, first is a straight taper and second is a non-linear taper. Straight tapers is the taper which have fixed angle and sudden discontinuity occurs at both end, in case of variable tapers, as name suggest angle is vary along length. In variable taper power converted into undesired mode is lower then straight taper [1]. Different types of basic waveguide tapers are shown in Fig. 2.6.

The non - linear taper for gyrotron is designed with high transmission coefficient (above 99%) with less unwanted mode generation. When output power is high so

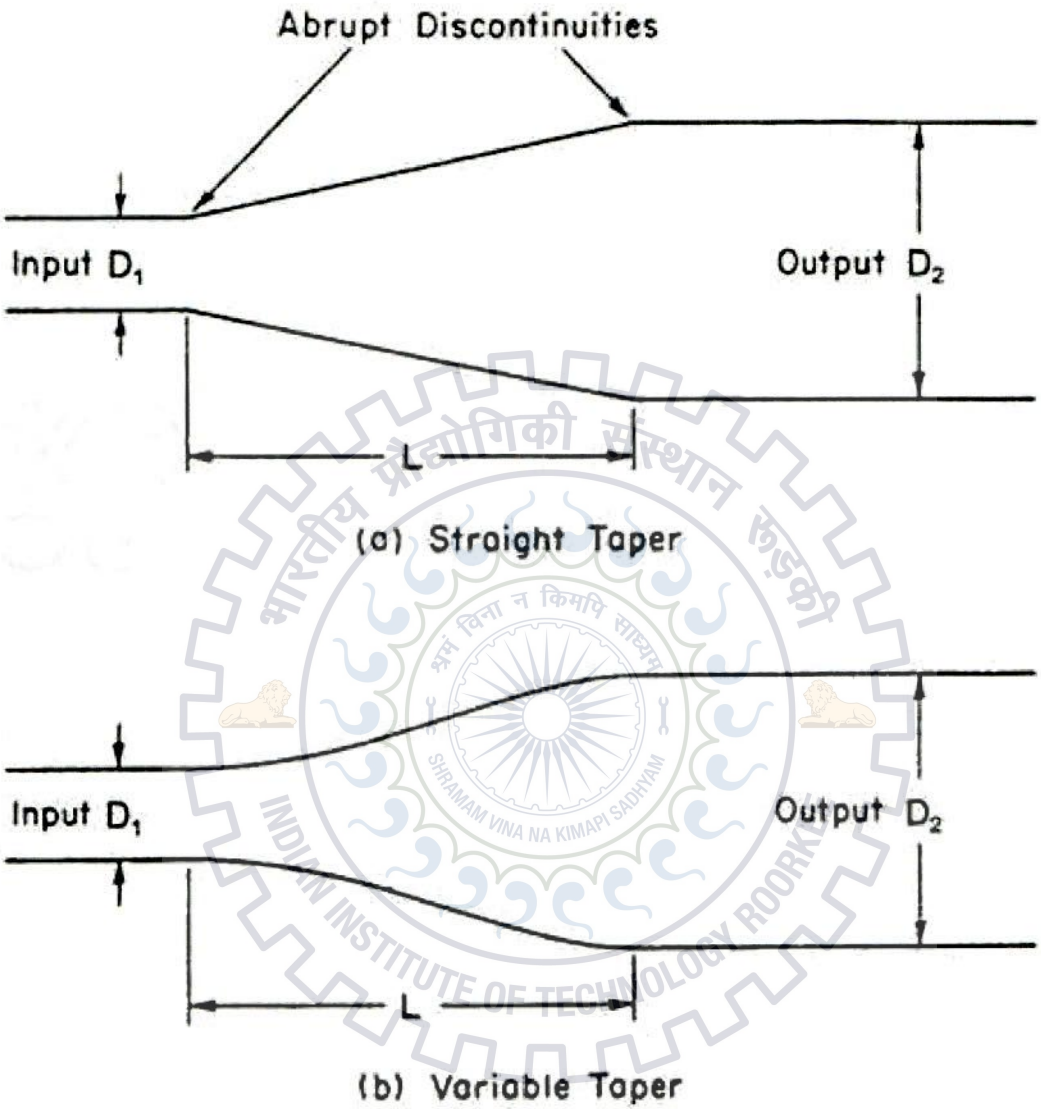

Figure 2.6: Different types of Tapers [1].

very less reflection can introduce damage in the system. That is why nonlinear taper should be design properly.

The main difficulties in the design of gyrotron output tapers in comparison with highly oversized waveguide tapers are as follows:

- Input reflections as well as forward and backward scattered waves must be

considered at the taper input, as the working mode is very close to cut off.

- The ratio of the collector to the cavity output radii is very large for conventional gyrotrons with axial output coupling. This can lead to a strong excitation of many parasitic modes.

- Mode coupling occurs as higher order working modes tend to couple to higher and lower undesired neighboring azimuthally symmetric modes. TE_{mn} modes with $n > 0$ couple not only to TE_{mq} modes but also excite TM_{mq} modes.

The presence of a taper in a waveguide introduces unwanted parasitic modes. Gyrotron output tapers should act as a near perfect match at the input port with suppressed spurious modes at the output port with a taper length as short as possible. Conical tapers with constant cone angle introduce a higher degree of parasitic modes which is not preferable. Tapers with gradual change in the cone angle cause considerably less power conversion to spurious modes. Since all the gyrotron output tapers are cylindrically symmetric, their performance does not depend on the sense of the rotation of the mode. The principle methods employed for the analysis and synthesis of gyrotron output tapers are given in detail in [1].

In the present work, a raised–cosine profile has been used for the taper design. A raised–cosine taper is given in Fig. 2.7. The synthesis of this taper profile was carried out using the following formulae [45]:

$$\alpha = -1.0 + 2.0 \left(\frac{i}{l}\right)^{\gamma} \tag{2.35}$$

$$r(z) = \frac{r_2 - r_1}{2} \cdot \left(\alpha + \frac{1}{\pi} sin(\pi\alpha)\right) + \frac{r_2 - r_1}{2} \tag{2.36}$$

$$r = r_1 + r(z) \tag{2.37}$$

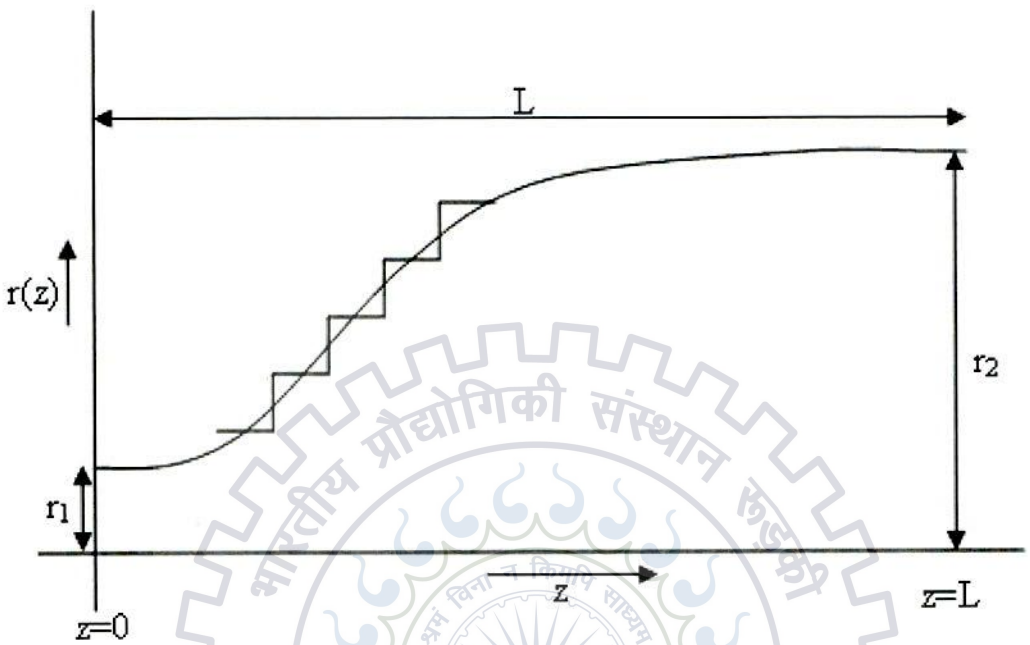

Figure 2.7: The raised–cosine taper profile

2.3.4 Quasi Optical (QO) Mode Converter

In the gyrotron, the quasi optical mode converter has a waveguide launcher, a quasi parabolic or elliptical mirror and one or two toroidal mirrors as shown in Fig. 2.8. The qo mode converter is inserted between cavity and RF window This Q-O launcher is used to convert cavity modes into a gaussian beam.

A simple example of quasi optical launcher is a Vlasov type launcher, it has a cylinder in which a cut along a helix. A Vlasov–type converter has a simple structure however, it suffers high diffraction loss (15%–20%) at its opening because the beam profile that is formed has a uniformly distributed field in the axial and azimuthal directions at the aperture.

A brief analysis of the quasi–optical launcher can be done as follows, for details refer [47] and the references therein.

A zero azimuthal E field at the waveguide wall define its relevant phase. In geometric

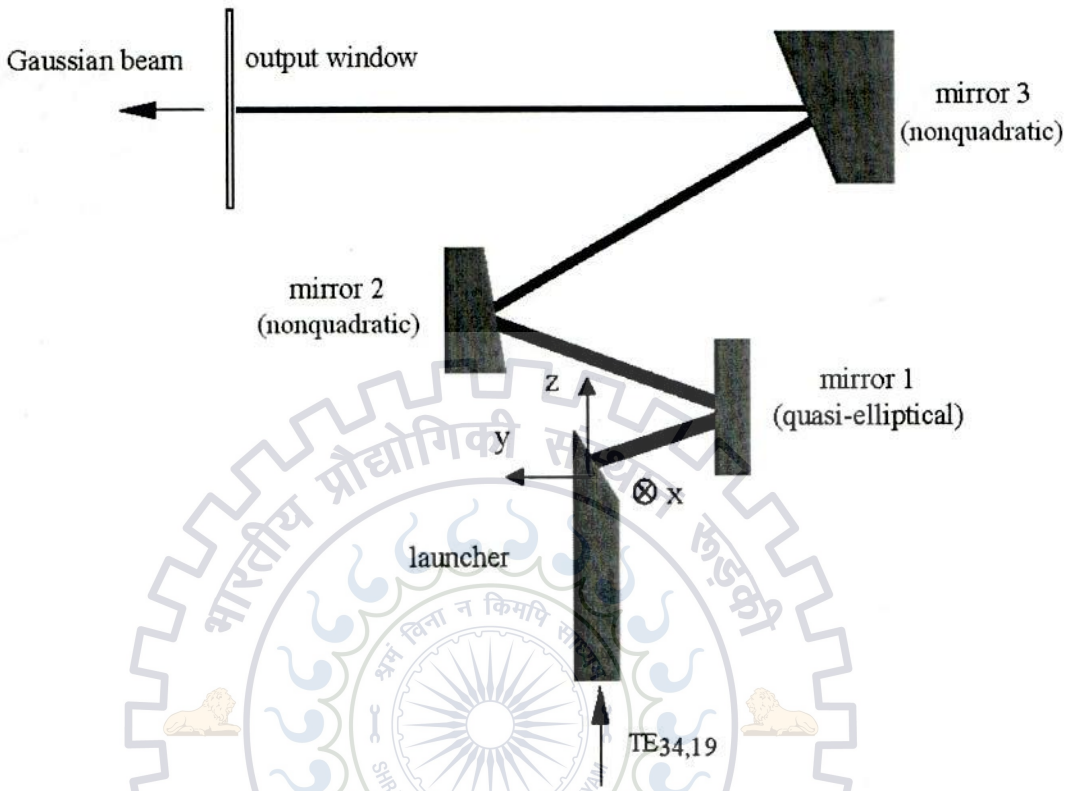

Figure 2.8: Schematic of the Quasi-optical RF output system [46].

optic limits, a simple wavefront is denoted by one ray. Its location is derived on the basis that the ray direction must coincide with the Poynting vector direction. If point is located in wall of waveguide so ray should have distance R_c given in equation 2.38 from the center of waveguide .

$$R_c = \frac{m}{x_{mn}} R_w \tag{2.38}$$

So if plane waves are presented by geometric optics ray formed a caustic of radius R_c. Now distance that a ray propagates in the axial direction between two reflection from the wall of waveguide is [48]:

$$L_B = 2R_w \left[1 - \left(\frac{m}{x_{mn}}\right)^2\right]^{1/2} \cot\theta_B \tag{2.39}$$

In transversal direction angle is given by:

$$\Delta\phi = 2\theta = 2\arccos\left(\frac{m}{x_{mn}}\right) \tag{2.40}$$

reflect all rays for one time. According to this reflections point of each rays is placed on the waveguide surfaces in a helical line with inclination angle

$$\alpha = \arctan\left(\theta \tan\theta_B / \sin\theta\right) \tag{2.41}$$

distance (pitch) that a ray has propagates in the axially when turns are:

$$H = 2\pi R_w \cot\alpha = 2\pi R_w \frac{k_z}{k_\perp} \frac{\sqrt{1-(\frac{m}{x_{mn}})^2}}{\arccos(\frac{m}{x_{mn}})} = L_c \tag{2.42}$$

which describe as launcher cut-length. Hence section of waveguide with length L_c described as $\Delta\phi R_w$ reflects each ray .

The surface deformation point on type two surface is calculate on method given by Hirata [47]. This deformation point is used for transformation of cavity mode into a group of modes which forms a gaussian profile. These points are optimized for maximum gaussian content in beam at helical cut. This converter is defined by the wall perturbation:

$$R(\phi, z) = a + \delta_1 \cos(\Delta\beta_1 z - l_1\phi) + \delta_2 \cos(\Delta\beta_2 z - l_2\phi) \tag{2.43}$$

where,

$$\begin{aligned} \Delta\beta_1 &= k_{zm,n} - k_{zm\pm1,n}, l_1 = \pm 1 \\ \Delta\beta_2 &= k_{zm,n} - k_{zm\pm\Delta m,n\pm\Delta n}, l_2 = \pm\Delta m \end{aligned} \tag{2.44}$$

Here, $k_{zm,n}$ is the longitudinal wave number for $TE_{m,n}$ mode, m and n are the azimuthal and radial index. The required minimal launcher length is

$$L_{min} = \frac{\pi}{|2\beta_{m,n} - \beta_{m+1,n} - \beta_{m-1,n}|} \tag{2.45}$$

2.3.5 RF–Window

As gyrotron is a high power source that operates at a very high frequency, high power levels and good pulse lengths, hence the transmission line system from gyrotron to plasma must be designed to handle these with low losses and low reflection back to the gyrotron [40]. Presently, heating power/pulse length that can be delivered to the industrial application is limited by the performance of the window.

Figure 2.9: Diamond CVD disc before installation into a gyrotron "Star-of-FZK" [1].

RF-window is classified in to main three categories.

- Single disk window
- Double disk window
- Brewster window

Single disk window is used to provide transmission for single frequency band. Brewster window provides better transmission for wide frequency band. So, it is most

suitable window for multi-frequency gyrotrons. Brewster window works only frequency range between 110 to 150 GHz. Double disk window is suitable for dual band gyrotron. Now CVD which is described as chemical vapor deposition diamond and BN CVD are used for formation of simple, single–disc windows. Disks grown by the chemical vapor deposition (CVD) technology should have exclusive combination of properties:

- a very high heat conductance.
- small microwave losses.
- modest dielectric constant
- low mm–wave attenuation ($tan\delta \approx 2 \times 10^{-5}$).
- mechanical resistance.

2.3.6 Collector

Most of the gyrotron collectors are designed in a way that the electron beam follow adiabatic diverge magnetic field line of gyrotron magnet with a diameter where the power is low so that remaining beam power will safe dissipated. The efficiency of microwave generation at high frequencies can be increased by float collector at a highly negative voltage [49].

The electron beam, after transfer of kinetic energy in RF energy is decelerated by a retarded E field before arrival at collector, this decelerate beam energy is gained by the power supply, which improve gyrotron efficiency very effectively.

Efficiency may be further increased by spatially splitting the spent electron beam into several energetic fractions. Then each of the fractions should be collected at an electrode of a retarding potential.

2.4 GDS V3 2014

A user friendly Graphical User Interface package "GDS V3 2014" (Gyrotron Design Suit for Fundamental Harmonic Version 3) is developed for the design of a gyrotron by cumulative efforts of members of millimeter wave laboratory with motivation and prevoyance of prof. M. V. Kartikeyan. It is an updated version of GDS V.01 [50]. It is a generalize package can be used for designing and conceptualize specific gyrotrons. This graphical user interface has been developed in MATLAB. It incorporates the specific procedure for selection of modes, starting current calculation, coils, resonator design and RF behavior calculations, launcher design, nonlinear taper design and single disk and double disk window design with user friendly interface. The Updated version of GDS V.01 also includes PSO optimization for Self C calculation, Non linear taper and capability of processing of very higher order modes with dual digit radial component. The new V3 has features to retrieve the phase of output beam and designing the profiles of mirrors as internal and external mode purifier.

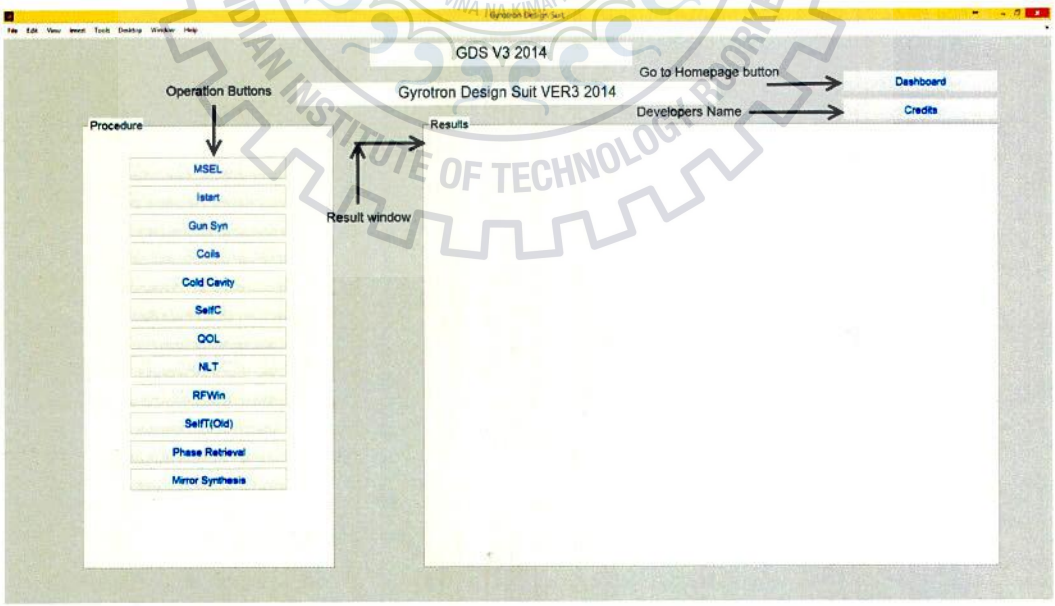

Figure 2.10: Dashboard of Gyrotron Design Suite.

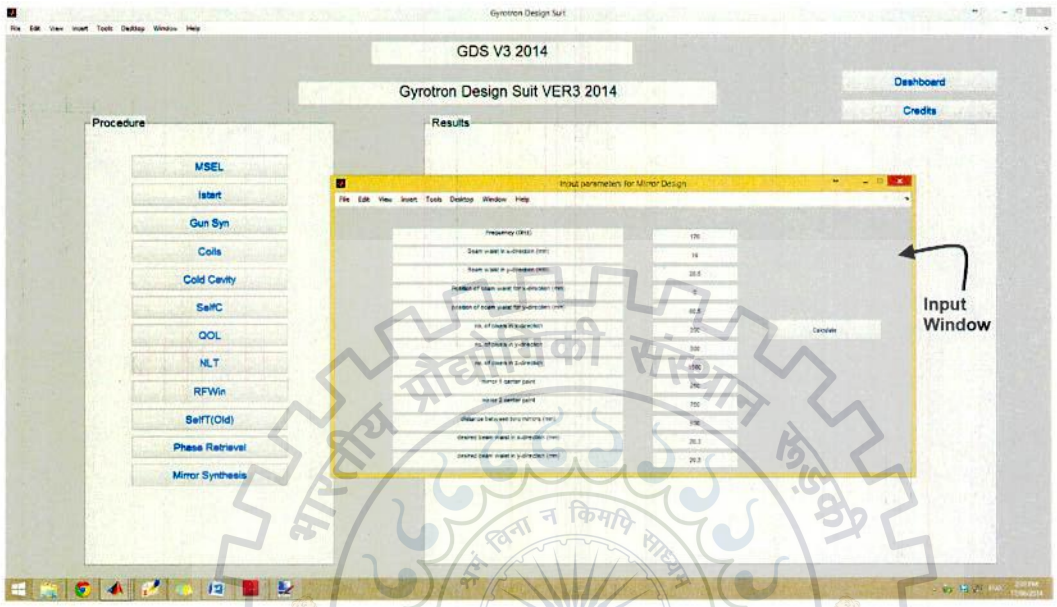

Figure 2.11: Mirror Synthesis input window

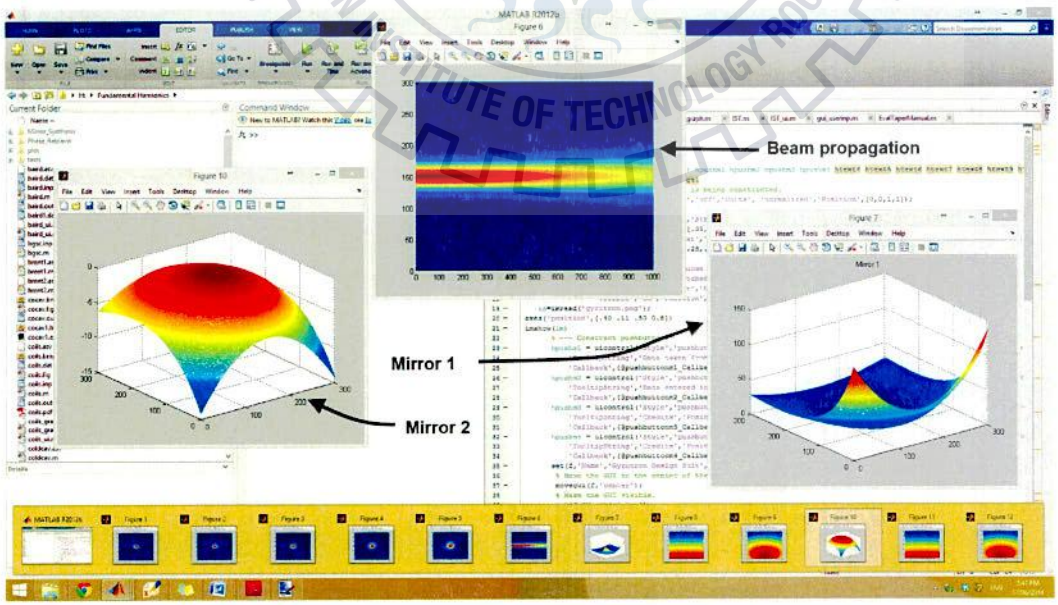

Figure 2.12: Mirror Synthesis results window

Chapter 3

Design Studies of 170 GHz, MW class CW Gyrotron

3.1 Mode Selection

The mode selection step is most important step in designing of gyrotron. These are the some points which should kept in mind to selecting a mode in gyrotron

1. Higher order volume modes realized.
2. Selection procedure should be carefully carried out, which will capable to giving high-quality solid beam output through a synthetic diamond window.
3. Mode selection involves the modes that support an advanced quasi-optical mode converter and less fundamental competitors.
4. Restriction the excitation of undesired modes.

For operation in the $TE_{m,n}$ mode, the cavity radius is related to λ by

$$R_0 = \chi_{m,n}\lambda/2\pi \tag{3.1}$$

where $\chi_{m,n}$ is the n^{th} root of $J'_m(x)$ The electron beam radius is usually chosen to maximize the coupling between the electron beam and the RF field. For fundamental

operation (S=1) the optimum electron beam radius is given by

$$R_b = \chi_{m\pm1,i}\lambda/2\pi \tag{3.2}$$

while for second harmonic operation (S=2) the optimum electron beam radius is given by

$$R_b = \chi_{m\pm2,i}\lambda/2\pi \tag{3.3}$$

Where (i=1 or 2)

In general, the corotating mode (with the lower sign) is chosen since this provides better coupling of the electron beam to the RF Field. The selected mode is $TE_{28,12}$

Table 3.1: Gyrotron Design Constraints

Parameter	Value
Peak ohmic wall loading (ρ_{wall})	$< 2KW/cm^2$
Voltage depression (Δ V /V)	< 0.1
Magnetic Compression ($b = B_{cav}/B_{gun}$)	< 50
Electric Field at the Emitter(E_e)	< 7 kV
Emitter mean radius (R_e)	< 50 mm
Cathode Current Density (j_e)	4.4 A/cm^2
Fresnel Parameter (C_F)	≈ 1.0

for the designing of this gyrotron.

3.2 Cold cavity design

The RF behavior analysis of gyrotron consist of mainly three steps:

- Conventional cavity is designed according to frequency and requirement to achieve desired Q value of cavity.
- Single mode self-consistence calculation is carried out to get optimum output power and efficiency of gyrotron for given beam parameter.

- RF behavior analysis is multi-mode time dependance calculation which involves analysis of output power with time in the presence of other competing modes.

This section includes cold-cavity design. Single mode and Multi-mode self-Consistence calculations will be carried out after MIG and magnetic guidance system design. The cavity is a standard three section structure with an input taper and a uniform mid section followed by an output up-taper. Parabolic smoothing of the input and output tapers is carried out to reduce unwanted mode conversion at sharp transitions. The input section is cutoff section which prevents the back propagation of RF wave to gun. The beam wave interaction takes place in the uniform mid section where the RF fields reach peak values. The uptakes with nonlinear contour connects the cavity with output waveguide and launcher of the quasi-optical output coupler.The external magnetic field starts to decrease in the uptakes region which results in residual interaction that sometimes causes a loss of efficiency. Therefore the output taper has not been included as a part of resonator geometry. Researchers are working to minimize after cavity interaction to improve efficiency. Table 3.2 shows a set of

Table 3.2: Interaction cavity data

Parameter	**set 1**	**set 2**	**set 3**	**set 4**	**set 5**
L_1 (mm)	14	14	14	14	14
L_2 (mm)	14	15	16	17	18
L_3 (mm)	14	14	14	14	14
$\theta_1(^\circ)$	2.5	2.5	2.5	2.5	2.5
$\theta_2(^\circ)$	0	0	0	0	0
$\theta_3(^\circ)$	2.5	2.5	2.5	2.5	2.5
D_1 (mm)	2.5	2.5	2.5	2.5	2.5
D_2 (mm)	2.5	2.5	2.5	2.5	2.5
Q_D (at 170 Ghz)	1166.7	1343	1549.9	1771.1	2020.8

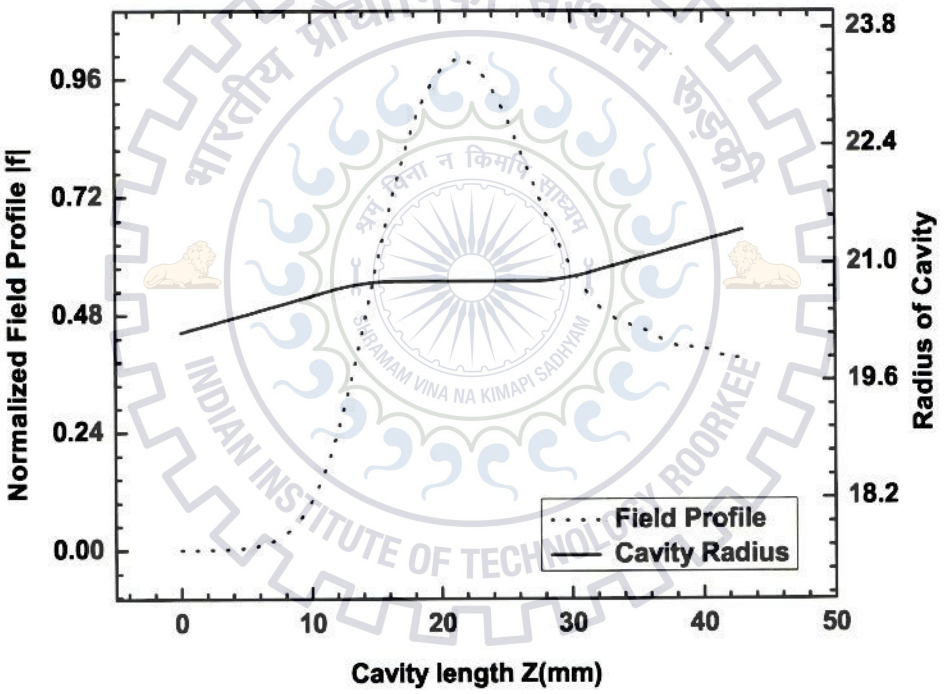

Figure 3.1: Cold cavity field profile at 170 GHz.

data for which cavity computations have been carried out. For $TE_{28,12}$ mode at 170 GHz, the cavity radius is 20.77 mm and beam radius is 8.27 mm. Computations has been done for cavity section's lengths L_1=14 mm, L_2=15 mm and L_3=14 mm that give values Q_D=1381 for $TE_{28,12}$ on the basis of reflection coefficient Γ=0.00018 and output frequency is 170.038 GHz.

3.3 Designing of magnetic guidance system

It is very important step in designing of gyrotrons. Magnetic field profile data are needed to perform precise simulation studies on magnetron injection gun and RF-behavioral aspects and also required for collector design. Efficiently designed Magnetic guidance system generates the maximum required uniform magnetic field at the center of the cavity and uses the stray field in the gun and collector region. To design such a magnetic guidance system most of the gyrotrons employ solenoids (either super-conducting or normal conducting coils) to provide necessary magnetic field for beam guidance from the cathode through interaction region up to the collector. A simple and cost effective magnet design can be achieved using a single coil while here we have used a radially tapered main coil (modeled by a single main coil and two auxiliary coils) and one gun coil to design a more effective guidance system. The setup of the magnetic guidance system is shown in Fig. 3.2. The initial data obtained from GDS V3, is then optimized using [51]. Here in our gyrotron design the required magnetic field is 6.725 Tesla for the fundamental operation at 170 GHz frequency. The change in the magnetic field is achieved by applying the proper current to the coils. For this gyrotron a diode type MIG is presented. The optimized coil data is tabulated in Table 3.3 for diode MIG.

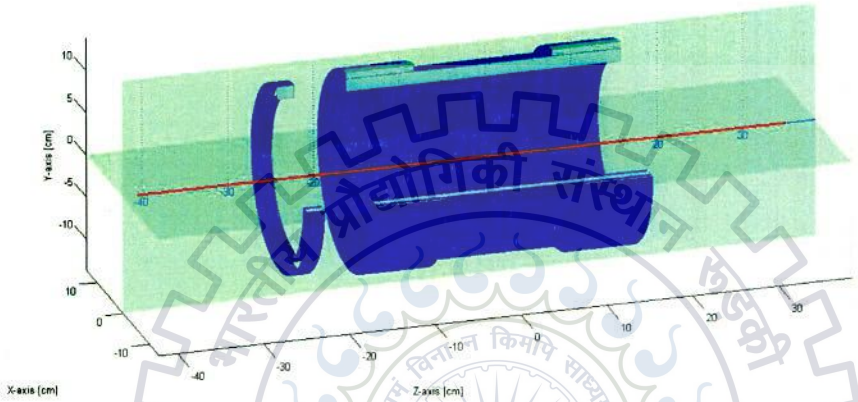

Figure 3.2: Magnetic field guidance system consists of main coil, auxiliary coil & gun coil.

Table 3.3: Magnetic guide system coils data for diode type MIG

Coils	Length (mm)	Radius (mm)	No. of Turns (N)	Current I (A)
Main Coil	340	15	20600	98
Aux. Coil-1	85	7.5	800	98
Aux. Coil-2	85	7.5	800	98
Gun Coil	25	15	995	-47.5

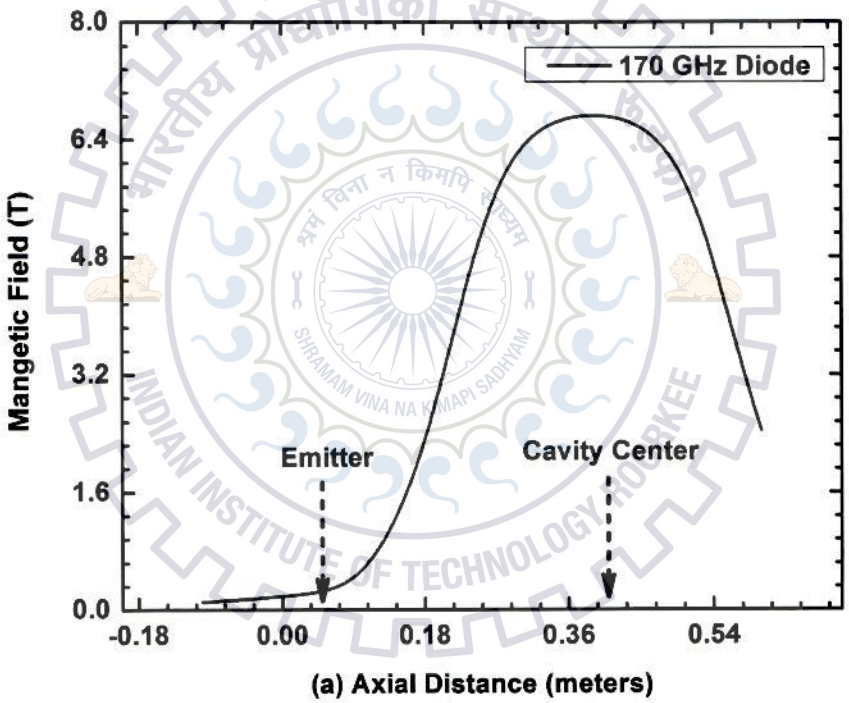

Figure 3.3: Magnetic field profile for diode MIG.

3.4 Designing of Magnetron Injection Gun

The term MIG refers to a class of electron guns in which thermionic emission arises from an axially symmetric cathode immersed in an axially symmetric magnetic field, arranged so that the axes of symmetry of the cathode and the field coincide. The parameters that decide the beam quality are velocity ratio ($\alpha = v_\perp/v_z$) and ($\beta = v_\perp/c$). In a gyrotron cavity resonator, the interaction is in between transverse electric fields and the transverse velocity of the electrons, hence α should be greater than one for a net energy transfer from beam to the wave. For high power levels and efficiency, an intense beam is required with a larger α and smaller velocity spread ($\Delta\alpha$). We require a high beam quality, the cathodes used in MIG's for gyrotrons are operated under temperature limited regime rather than in space-charge-limited to minimize the velocity spread in the beam.

Initial step of designing of the MIG is the calculation of the optimum beam radius and maximum magnetic field requirement. From resonator design calculations one has information about the magnetic field requirements in the cavity region, cavity radius and beam radius. Then, by making use of Baird's trade-off expressions [52] , one can compute the gun design parameters in adiabatic approximation, taking into account the technical and physical constraints, namely emitter radius, emitter current density, space charge ratio, cathode to anode distance, etc. These calculations are made with an initial beam voltage, beam current and velocity ratio taken from the cavity design. The design optimization is carried out using the ESRAY code. The final design values obtained after optimization are summarized in Table 3.4.

Designing of MIG is fist based on Busch's theorem [1]. From Busch's theorem the cathode radius is related to the beam radius (in paraxial approximation) by

$$R_c = \sqrt{b} R_b \tag{3.4}$$

Where R_c is cathode radius, R_b is the beam radius and b($=B_{cavity}/B_{gun}$) is the compression ratio. Designed MIG for for a particular frequency can be operated

Table 3.4: Preliminary Design Data of Diode-MIG.

Parameter	**Value for Diode-MIG**
Beam current	42 A
Accelerating Voltage	77 keV
Magnetic field at cavity	6.725 T
Magnetic field at gun	0.248 T
Compression ratio	27.12
Beam radius at interaction	8.295 mm
Relativistic mass factor (γ_0)	1.52
Larmour radius	0.088 mm
Cathode radius (R_C)	50.65 mm
Emitter radius (R_E)	44.23 mm
Anode radius	66.8 mm
Axial length of Emitter	3.8725 mm
Emitter current density	4.4 A/cm^2
Cathode-Anode spacing (dml)(R_{CM})	16 mm
Emitter-Anode spacing (perpendicular)	18.47 mm
Cathode angle	32°
β_z ($\Delta\beta_{Z_0}$)	0.364
$\beta_\perp$ ($\Delta\beta_\perp$)	0.303
Velocity ratio (α)	1.202
Velocity ratio spreading ($\Delta\alpha$)	2.986 %
E-field at cathode	$\approx$ 7.4 kV/mm
Max. wall loading	9.36×10^6 Watts/cm^2
Total absorbed power	2.91×10^6 Watts
E-kinetic [keV]	69.49

on other frequency by changing the value of B_{gun} which results a change in compression ratio(b) and achieved the desired guiding center radius($\neq$ Rb). For our operation R_b=8.273 mm, optimized velocity ratio (α=1.2) and minimum velocity spread ($\Delta\alpha \leq 5\%$).

A diode type of MIG consists of a ring emitter mounted over a cathode and an accelerating anode as shown in Fig. 3.4. A diode-type gun is preferred for applications which have stringent requirements on the power supply [53]. The beam trajectory is shown in Fig. 3.5.

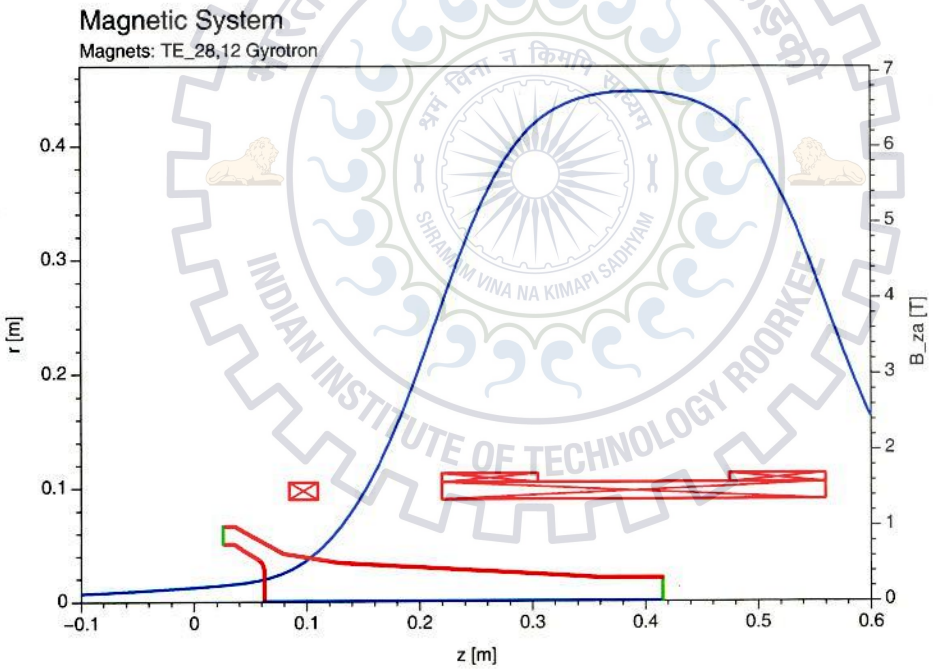

Figure 3.4: MIG geometry and magnetic field profile for diode MIG.

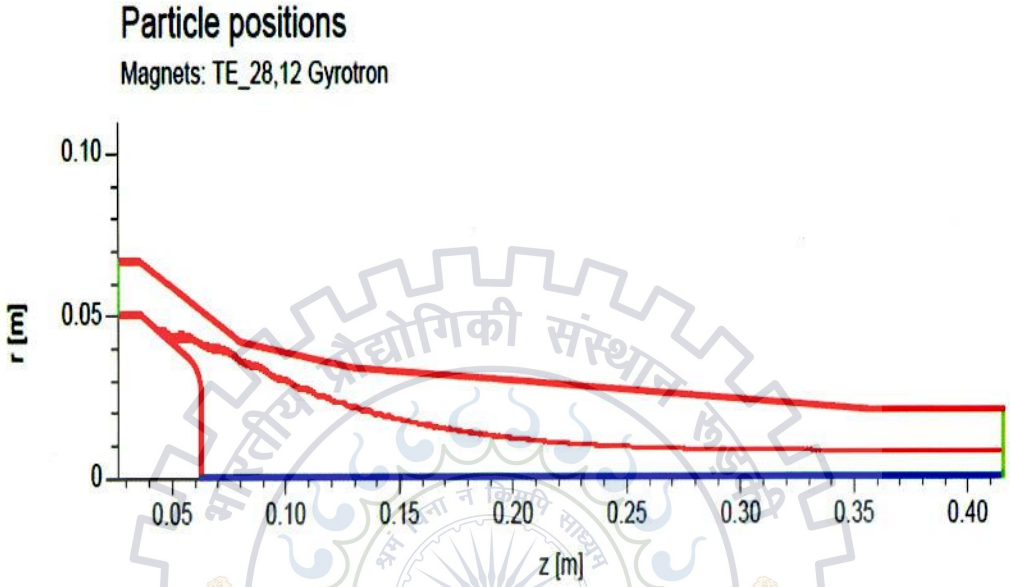

Figure 3.5: Beam trajectory for diode MIG.

3.5 Self - Consistent Calculations

Self-consistent calculations for power and efficiency are carried out for a range of external parameters, namely:

beam voltage, beam current and applied magnetic field. Computations are carried out for three cavity mid section lengths L_2 = 14.0/15.0/16.0/17.0/18.0 mm that give values of Q_D = 1166.7/1343/1549.9/1771.1/2020.8 respectively. The results of the cavity design based on self-consistent computations are shown in Figs. 3.6–3.9. These indicate the cavity geometry corresponding to Q_D = 1343 as the best choice. From these figures, it is evident that operation at the fundamental harmonic (s=1) at 170 GHz with the $TE_{28,12}$ mode as the operating mode gives well above 1200 kW of cavity output power with around 37% efficiency and minimum wall losses.

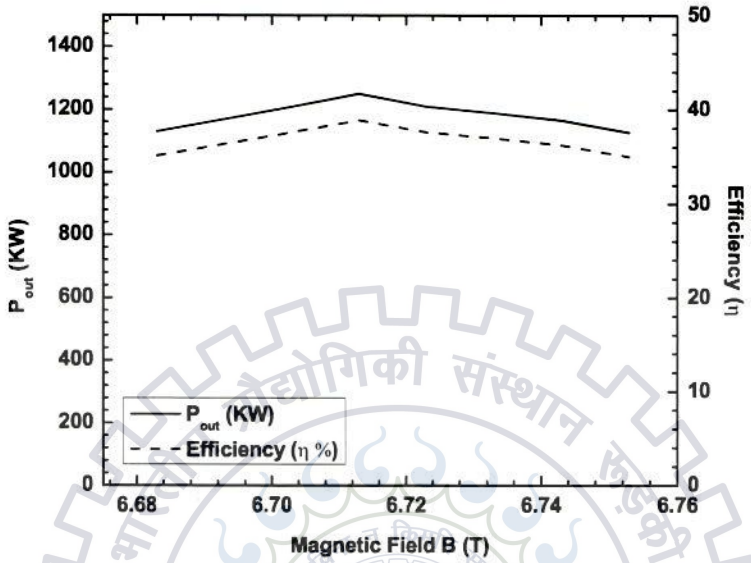

Figure 3.6: Cavity output power and efficiency as a function of cavity magnetic field (B_0) with U_b=77 kV, I_b=42 A and α=1.20.

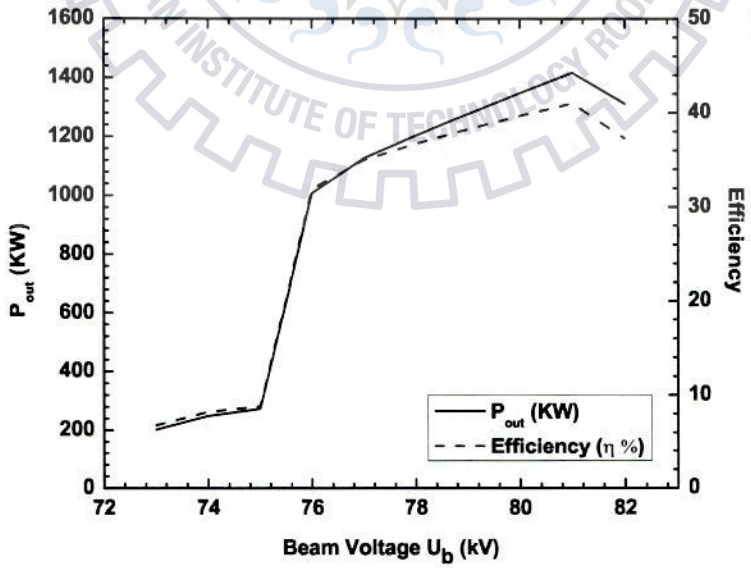

Figure 3.7: Cavity output power and efficiency as a function of applied beam voltage (U_b) with B_0=6.725 T, I_b=42 A and α=1.20.

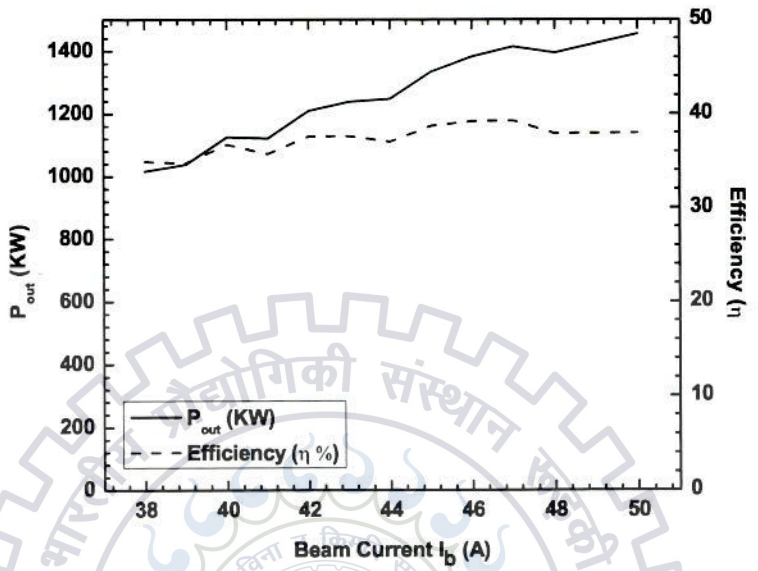

Figure 3.8: Cavity output power and efficiency as a function of applied beam current (I_b) with U_b=77 kV, B_0=6.725 T and α=1.20.

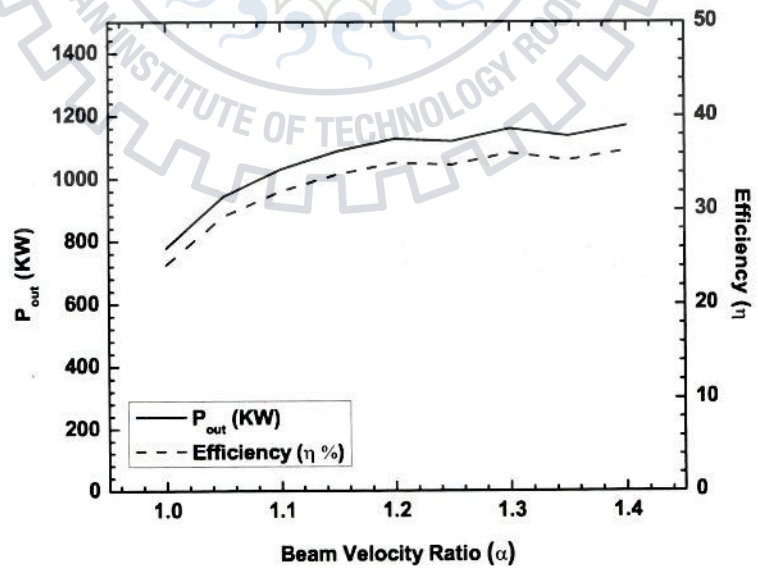

Figure 3.9: Cavity output power and efficiency as a function of beam velocity ratio (α) with U_b=77 kV, B_0=6.725 T and I_b=42 A.

3.6 Output System

3.6.1 Designing of Non linear taper

Table 3.5: NLT design values after optimization

R_1 (mm)	21.381
R_2 (mm)	23.1
Length L (mm)	165.76
No. of sections N	216
Shape factor γ	0.706
Transmission Coefficient (S_{21}) (at 170 Ghz)	99.50

In the NLT design section a non linear diameter taper of raised cosine type is presented which is connecting to the output section of gyrotron cavity to the uniform waveguide section. The requirement of a diameter taper in gyrotrons is to provide a good match between input and output sections of taper with very low spurious mode content. In this work, a non linear taper of raised cosine profile has been used as it yields very low mode conversion. The analysis of the taper was carried out using a dedicated scattering matrix code, and for the design optimization of the non linear taper, an improved particle swarm optimization (PSO) an evolutionary optimization algorithm has been used.

The objective of the design was to obtain a maximum transmission coefficient (i.e.,S_{21} parameter), operating with $TE_{28,12}$ mode at 170 GHz with minimized spurious mode content. Finally, taper contour profile along its length is appreciated graphically in Fig. 3.10. A transmission of 99.50 % at 170 GHz has been achieved.

3.6.2 Designing of Quasi optical launcher

The advanced mode converter consists:

- A dimpled wall waveguide section and a helical-cut launching aperture as an

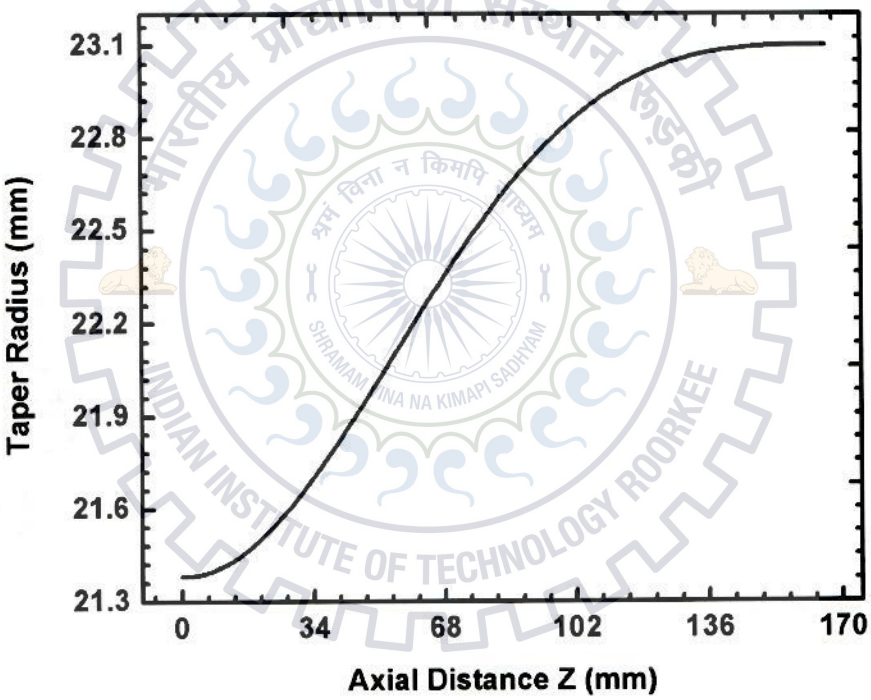

Figure 3.10: Non linear taper profile after optimization.

antenna.

- One quasi elliptical mirror and two toroidal mirrors as beam forming mirror system (Internal phase correctors).

Table 3.6: Launcher design parameters

Launcher length (mm)	220
Helical cut length (mm)	82
Waveguide radius (mm)	23.1
Taper angle (Rad.)	0.005

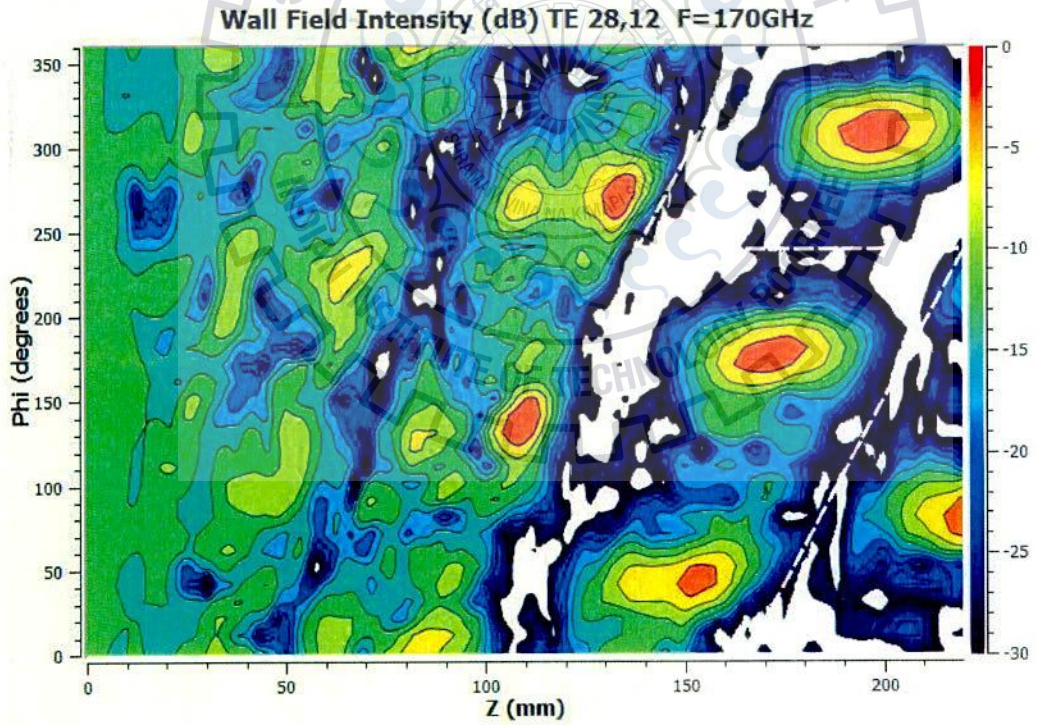

Figure 3.11: Wall Field intensity for $TE_{28,12}$ mode at 170 GHz.

There is a need for the conversion of higher order modes to gaussian like beam for better efficiencies. The deformations present on the scattering surface of the dimpled wall waveguide antenna can transform the input eigenwave to an eigenwave of the

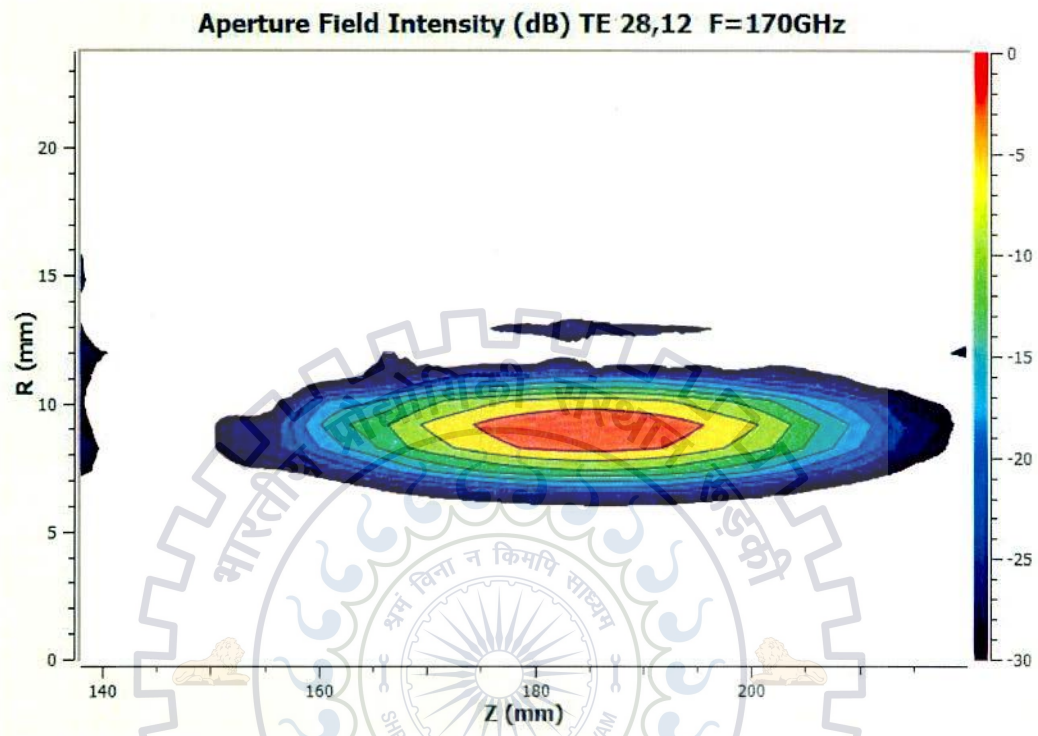

Figure 3.12: Aperture Field intensity for $TE_{28,12}$ mode at 170 GHz.

Table 3.7: Results for designed launcher

Gaussian content factor	99.68%
Energy conversion	99.58%

weakly perturbed transmission line. That beam is appropriate to be used directly as a free space TEM_{00} mode, or to be transmitted as a low-loss hybrid HE_{11} mode in highly over-moded corrugated waveguide. The launcher design parameters are presented in Table 3.6 and achieved results are in Table 3.7.

3.6.3 Designing of RF window

The RF vacuum window separates the vacuum of gyrotron from the outside atmosphere. It plays an important role in transmitting the output to the external system.

Table 3.8: Design values for single disk windows

Window material	Diamond	BN CVD
Window aperture radius (mm)	45	45
Disk thickness (d)(mm)	1.8529	2.4419
Disk dielectric constant ($\epsilon^{'}$)	5.67	4.7
Loss tangent	0.00004	0.00115
Transmission Coefficient (%)	99.9	97.2

The properties of a good window is:

- It must withstand in the high power.
- it should have ability to handle mechanical stresses and pressure gradients.
- Low loss tangent.
- High thermal conductivity and mechanical strength.
- Easy metallization/brazing and make a strong vacuum tight seal with metals.
- CVD Diamond is the material which is most suitable for the designing of window at high power level.

Single disk window is used to provide transmission for single frequency band. Brewster window provides better transmission for wide frequency band. So, It is most suitable window for multi frequency gyrotrons. Brewster window works only frequency range between 110 to 150 GHz. Double disk window is suitable for dual band gyrotron. The design values for single disk windows shown in Table 3.8. Fig. 3.13 and Fig. 3.14 shows transmission and reflection co-efficient for BN CVD and diamond type window respectively.

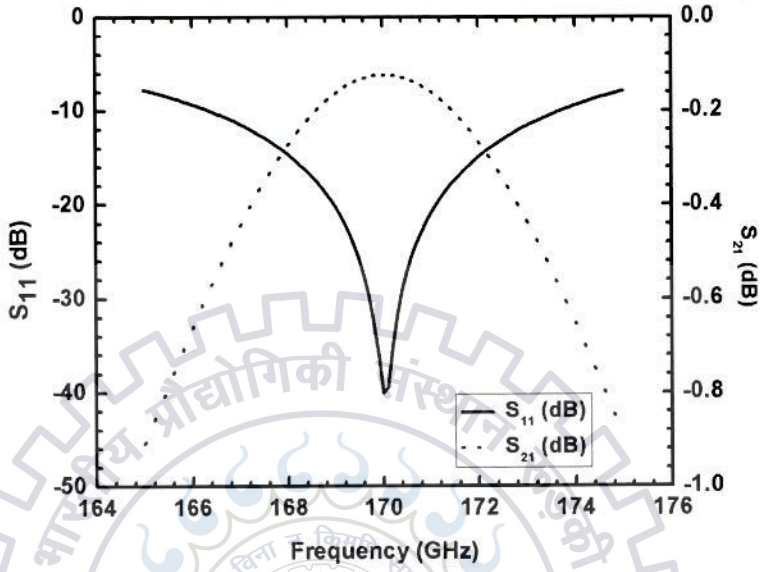

Figure 3.13: Reflection coefficient and transmission coefficient of designed RF window with BN CVD material for 170 GHz operation.

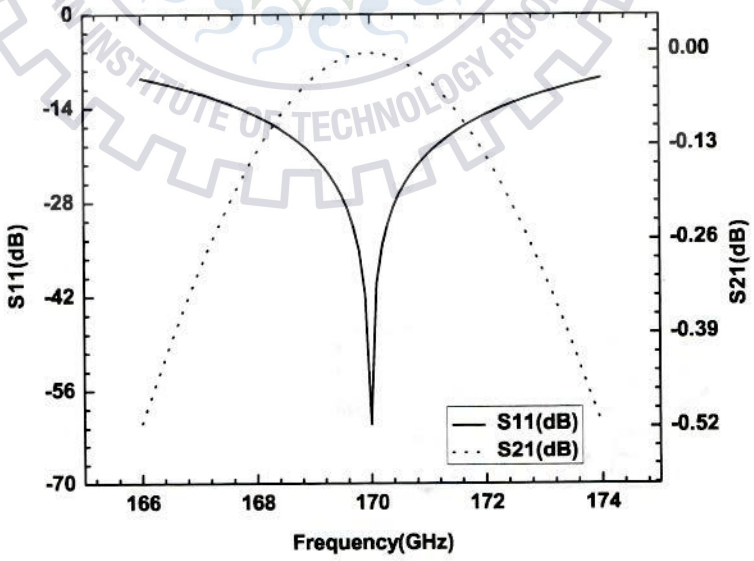

Figure 3.14: Reflection coefficient and transmission coefficient of designed RF window with diamond material for 170 GHz operation.

Chapter 4

Phase Retrieval and Mirror Synthesis

4.1 PHASE RETRIEVAL ALGORITHM

4.1.1 Introduction

In this chapter, the concept of reconstruction of phase is explained. The Algorithm Iterative Phase Retrieval Algorithm(IPRA) is explained. The problem of phase retrieval from two intensity measurements (in beam investigation of gyrotron and electron microscopy or wave-front sensing) [54]. Our goal is to design the phase correcting reflectors of a gyrotron which are accurate and reliable. The surface profile of these reflectors shape the output microwave beam by correcting for aberration in the phase front [55]. For analysis and synthesis of these mirrors, we require the knowledge of phase and amplitude both [56]. Phase can not measured directly at higher frequencies in the labs, so we need to formulate the phase from the measured intensity pattern. We wish to develop an accurate and reliable method to retrieve the phase of a gyrotron gaussian-like beam from a series of intensity measurements. There are two or more amplitude distributions along the direction of propagation is given with the help of these phase must be retrieve. Once the phase is known, we

can predict the waves behavior at any point. This process is useful in designing the phase-correcting reflectors of the gyrotron.

4.1.2 Iterative Phase Retrieval Algorithm

Iterative Phase Retrieval Algorithm(IPRA) is also known as Gerchberg - Saxton algorithm [57] was originally invented in connection with the problem of reconstructing phase from two intensity measurement [54]. We take the measure intensity planes. The number of planes can be several. We are taking two planes i and j as shown in Fig. 4.1 (a). The method consists of 6 steps

1. Assume initial phase, multiply it with the measured intensity at plane 1.
2. Propagate it with any propagator to plane 2, calculate intensity and phase at plane 2.
3. Replace computed amplitude with the measured amplitude of plane 2.
4. Back propagate it to the plane 1 using same propagator.
5. Replace the measured amplitude at plane 1.
6. Repeat the above process until the error reaches to the required threshold.

Forward Propagation

The EM field of a wave at i^{th} plane can be written as

$$F_i(x, y, z_i) = A_i(x, y) \exp\left[i\phi_i(x, y)\right] \tag{4.1}$$

Where, $A_i(x, y)$ and $\phi_i(x, y)$ are wave amplitude and phase at the i^{th} plane respectively. The field F_i after distance Z_i is given as

$$F_j(x, y, z) = F^{-1}\left\{\exp\left[i\left(z_j - z_i\right)k_z\right] \times F\left[u_i(x, y, z)\right]\right\} \tag{4.2}$$

Where, k_z is wave number and F and F^{-1} denotes the Fourier Transform and its inverse respectively [59]. Figure 4.1 shows the Iteration method. If the wave

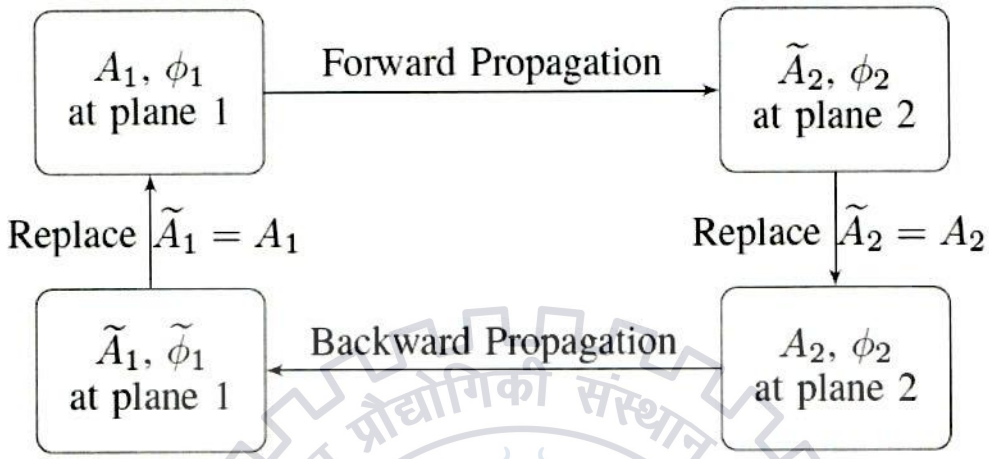

Figure 4.1: Algorithm of Phase reconstruction in two cross sections. A_1, A_2 and $\tilde{A}_1$, $\tilde{A}_2$ are the measured and calculated fields in the two planes Z_1 and Z_2 respectively [59].

propagation happening in z-direction, taking x, y plane, at the later distance z_i the generalize field expression can be written as

$$F_j(x', y') = \int\int_{\Omega} F_i(x, y)\, P(x' - x\ ,\ y' - y)\, dx\, dy \tag{4.3}$$

Where, (x,y) represents the input plane coordinates and (x', y') represents the output plane coordinates at Z_i and Z_j plane respectively. P$(x' - x\ ,\ y' - y)$ is the propagator used to propagate the field from the plane at Z_i to Z_j and Ω is the region of input plane [58].

Backward Propagation

The new field at plane Z_j have the $\tilde{A}_2$ and ϕ_2 amplitude and phase respectively. $\tilde{A}_2$ is replaced by A_2. The field is now back propagate from Z_j to Z_i using the propagator which is the complex conjugate of the forward propagator. At plane Z_i new field will have now $\tilde{A}_1$ and ϕ_1 amplitude and phase respectively, then $\tilde{A}_1$ is replaced by old amplitude A_1.

Propagators

The propagators here used can be directly Green function and Huygens - Fresnel propagator as this is for the calculation of near field. So, green function for this method

$$P\left(x'-x,y'-y\right)\rightarrow G_{i\rightarrow j}\left(x'-x,y'-y\right) \tag{4.4}$$

$$G_{i\rightarrow j}\left(x'-x,y'-y\right)=\frac{1}{2\pi}\frac{\partial}{\partial z}\left(\frac{\exp\left(ikr\right)}{r}\right) \tag{4.5}$$

or it is nearly equals to

$$G_{i\rightarrow j}\left(x'-x,y'-y\right)=\frac{2\Delta z}{r}\left(ik-\frac{1}{r}\right)\frac{\exp\left(ikr\right)}{4\pi r} \tag{4.6}$$

Where k is the wavenumber given in terms of wavelength λ by $k=2\pi/\lambda$, $\Delta z=(z_j-z_i)$ and $r=\left[\left(x'-x\right)^2+\left(y'-y\right)^2+\left(\Delta z\right)^2\right]^{\frac{1}{2}}$.

Huygens-Fresnel propagator,

$$h_{i\rightarrow j}\left(x,y\right)=\frac{1}{i\lambda\Delta z}\exp\left\{i2\pi\frac{\Delta z}{\lambda}\right\}\exp\left\{i\pi\frac{x^2+y^2}{\lambda\Delta z}\right\} \tag{4.7}$$

4.1.3 Error, Iteration, Advantages and Disadvantages

The criterion to stop the iteration is when error reaches to

$$E_j^{(n)}=\int_{S_j}\left|A_j-A_j^{(n)}\right|^2 ds_j<\epsilon_j \tag{4.8}$$

Where, n is the number of iterations and ϵ_j is a set of small error values, S_j is surface in which the integral is performance. Advantages of this is it is more accurate in general case of gyrotrons [59], can use to calculate for high fraction of higher order modes [59]. The disadvantages are the initial choice affects the result plane separation and plane dimension are fixed, For large errors method does not converse to a solution.

4.1.4 IPRA Results and Discussion

To show the phase reconstruction mechanism an arbitrary amplitude contours have been taken as shown in Fig. 4.2. The Fig. 4.2 (a)-(d) shows amplitude contours

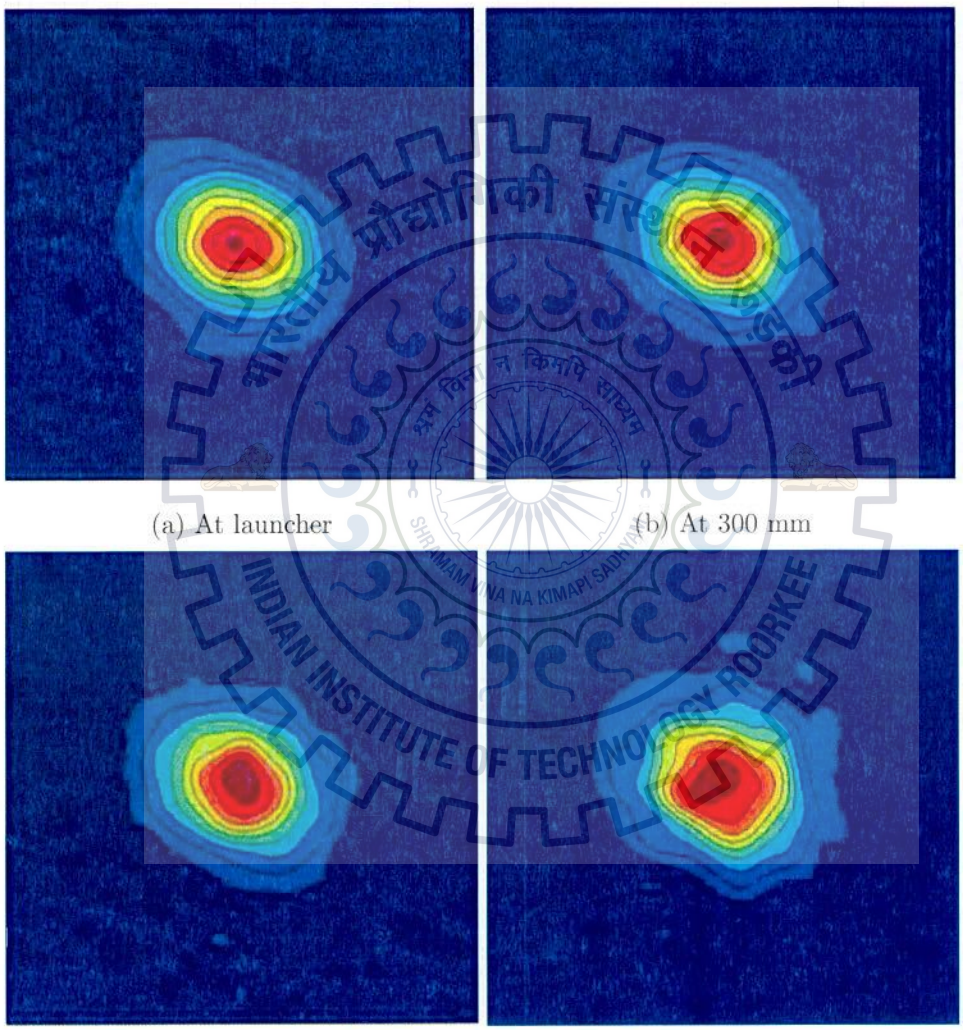

(a) At launcher (b) At 300 mm

(c) At 600 mm (d) At 900 mm

Figure 4.2: Amplitude contours for different separations from window

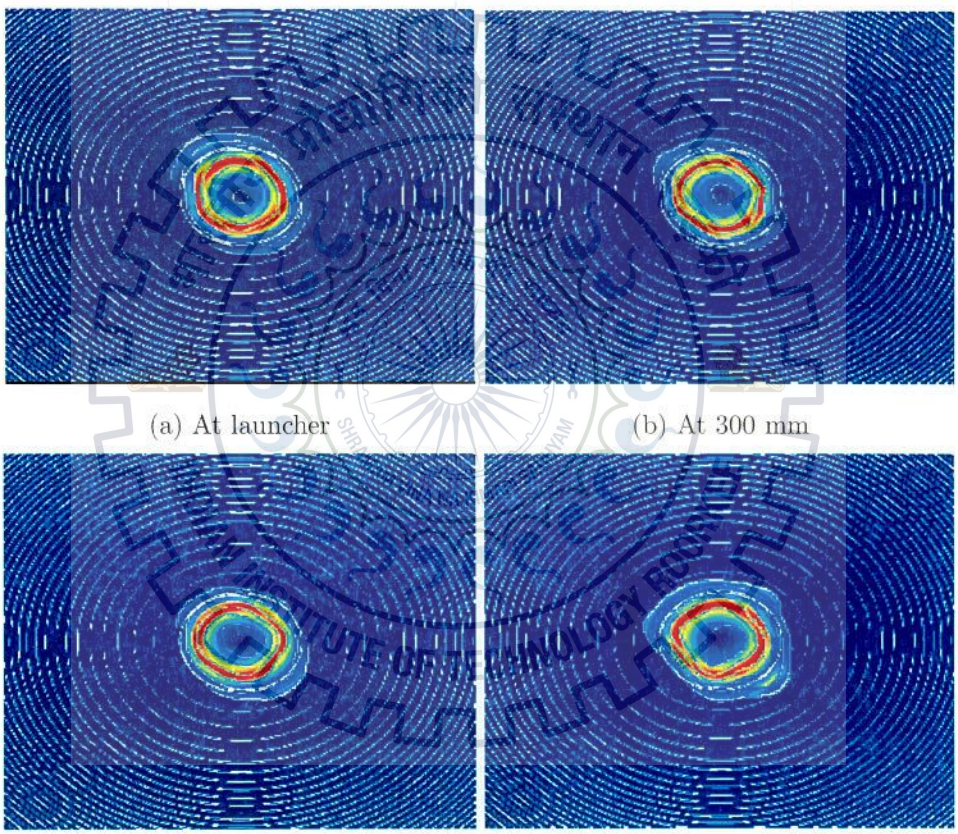

(a) At launcher (b) At 300 mm

(c) At 600 mm (d) At 900 mm

Figure 4.3: Phase contours for different separations from window

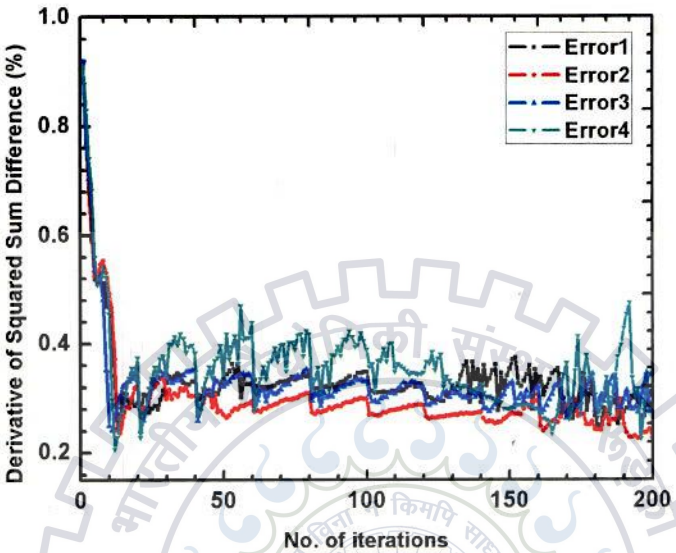

Figure 4.4: Error (%) v/s No. of iterations (i) Error1 at plane 1, (ii) Error2 at plane 2, (iii) Error3 at plane 3, (iv) Error4 at plane 4.

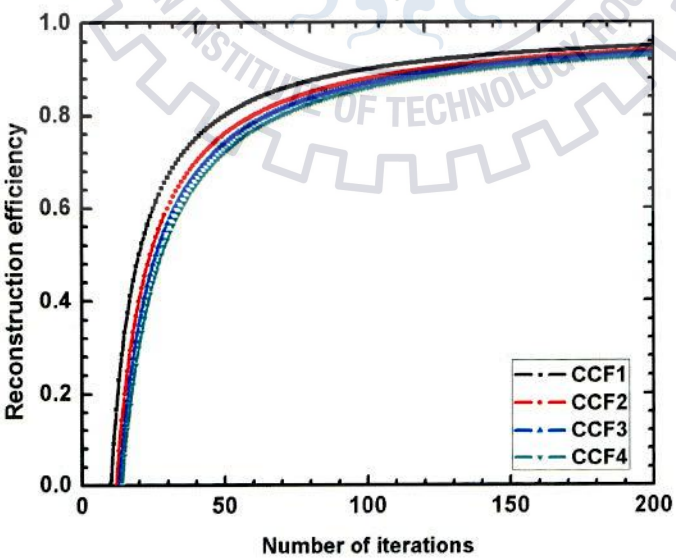

Figure 4.5: Cross co-relation Factors (i) CCF1 at plane 1, (ii) CCF2 at plane 2, (iii) CCF3 at plane 3, (iv) CCF4 at plane 4.

at different separation from the window. The corresponding reconstructed phase is shown in Fig. 4.3. The Error and Cross correlation factors are shown in Figs. 4.4 and 4.5 respectively. These parameters represents the effectiveness of IPRA.

4.2 Mirror Synthesis

Based on the method given in [60] two mirrors system designed for MOU. The equations are as follows:

$$u_{00} = \sqrt{\frac{2}{\pi w_x w_y}} \exp\left(-\frac{(x-x_0)^2}{w_x^2} - \frac{(y-y_0)^2}{w_y^2} - j\phi\right) \tag{4.9}$$

The above equation used to produce the Gaussian-like beam. The equation 4.10 represents the phase distribution of Gaussian beam.

$$\phi = kz + \frac{\pi\,(x-x_0)^2}{\lambda R_x} + \frac{\pi\,(y-y_0)^2}{\lambda R_y} - \frac{\phi_{0x}}{2} - \frac{\phi_{0y}}{2} \tag{4.10}$$

The equation 4.11 and 4.12 represents the beam waists in the x and y direction for different value of z (direction of propagation).

$$w_x = w_{0x}\sqrt{1 + \left(\frac{\lambda\,(z-z_{0x})}{\pi w_{0x}^2}\right)^2} \tag{4.11}$$

$$w_y = w_{0y}\sqrt{1 + \left(\frac{\lambda\,(z-z_{0y})}{\pi w_{0y}^2}\right)^2} \tag{4.12}$$

The equation 4.13 and 4.14 represents the beam radii in the x and y direction for different value of z (direction of propagation).

$$R_x = (z-z_{0x}) + \frac{1}{(z-z_{0x})}\left(\frac{\pi w_{0x}^2}{\lambda}\right)^2 \tag{4.13}$$

$$R_y = (z-z_{0y}) + \frac{1}{(z-z_{0y})}\left(\frac{\pi w_{0y}^2}{\lambda}\right)^2 \tag{4.14}$$

The equation 4.15 and 4.16 represents the beam waists in the x and y direction for the value of z=0.

$$\phi_{0x} = \tan^{-1}\left(\frac{\lambda\,(z-z_{0x})}{\pi w_{0x}^2}\right) \tag{4.15}$$

$$\phi_{0y} = \tan^{-1}\left(\frac{\lambda\left(z - z_{0y}\right)}{\pi w_{0y}^2}\right) \tag{4.16}$$

The equations 4.17 - 4.20 gives the information of phase of incident and reflected beam at the mirror. Where $\Delta\phi_{in}$ and $\Delta\phi_{out}$ are the change in input and output phase respectively.

$$\phi_{in} = \phi_{cin} + \Delta\phi_{in} = \left(\frac{\phi_{0xin} + \phi_{0yin}}{2}\right) - kz - \frac{k}{2}\left(\frac{\left(x - x_0\right)^2}{R_{xin}} + \frac{\left(y - y_0\right)^2}{R_{yin}}\right) \tag{4.17}$$

$$\phi_{cin} = -kz_c = +\frac{1}{2}\left(\tan^{-1}\left[\frac{\lambda\left(z_c - z_{0xin}\right)}{\pi w_{0xin}^2}\right] + \tan^{-1}\left[\frac{\lambda\left(z_c - z_{0yin}\right)}{\pi w_{0yin}^2}\right]\right) \tag{4.18}$$

$$\phi_{out} = \phi_{cout} + \Delta\phi_{out} = \left(\frac{\phi_{0xout} + \phi_{0yout}}{2}\right) - kz - \frac{k}{2}\left(\frac{\left(x - x_0\right)^2}{R_{xout}} + \frac{\left(y - y_0\right)^2}{R_{yout}}\right) \tag{4.19}$$

$$\phi_{cout} = -kz_c = +\frac{1}{2}\left(\tan^{-1}\left[\frac{\lambda\left(z_c - z_{0xout}\right)}{\pi w_{0xout}^2}\right] + \tan^{-1}\left[\frac{\lambda\left(z_c - z_{0yout}\right)}{\pi w_{0yout}^2}\right]\right) \tag{4.20}$$

To get the mirror profile, the results comes out by the above four equation put in the equation 4.21.

$$S\left(x, y, z\right) = \frac{\Delta\phi_{out} - \Delta\phi_{in}}{2k\cos\beta} = \frac{\left(\phi_{out} - \phi_{cout}\right) - \left(\phi_{in} - \phi_{cin}\right)}{2k\cos\beta} \tag{4.21}$$

In MOU the center position of mirrors is 250 mm and 750 mm from the gyrotron window. The separation between them is 500 mm and the angle with the incident beam is 45°. Fig. 4.6 shows the schematic arrangement of the mirrors in MOU. The obtained mirror profiles for the mirrors are shown in Figs. 4.8 and 4.9. The axial view or normalized field intensity in the axial direction at beam center of propagating

wave beam is shown in Fig. 4.7. The incident beam at the mirror 1 has 19 mm and 20.5 mm beam waists in x and y direction respectively. The beam has astigmatism in the z direction of 60.5 mm. After correction of beam ellipticity the beam waists are 20.3 and 20.31 in the x and y direction respectively. The ellipticity of beam is corrected from 1.133 to 1 while the astigmatism corrected from 60.5 mm to 3.25 mm. After obtaining this results the beam will have better coupling efficiency with the corrugated waveguide of 63.5 mm diameter. In Table 4.1 shows the incident and output beam parameters.

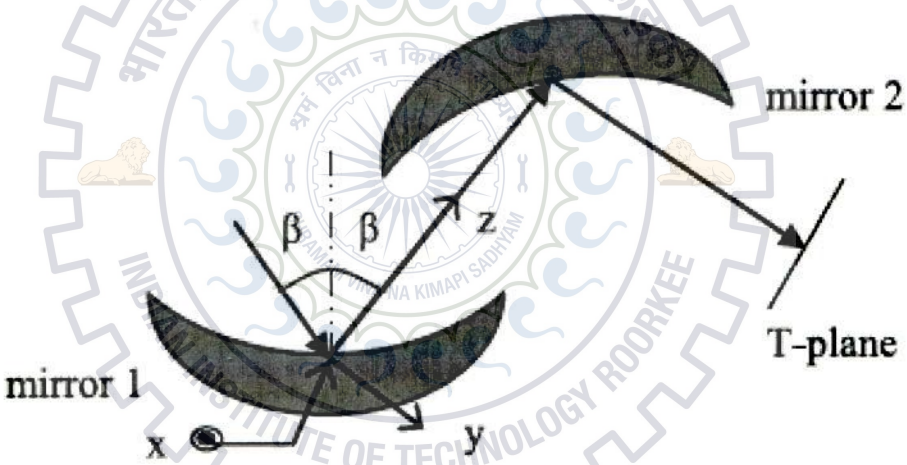

Figure 4.6: Schematic arrangement of beam shaping mirrors in MOU [60].

Table 4.1: Input, Output wave beam parameters for MOU

Parameter	Incident beam	Output beam
w_{0x} (mm)	19	20.3
w_{0y} (mm)	20.5	20.31
z_{0x} (mm)	0	910
z_{0y} (mm)	60.5	913.25
Ellipticity ζ	1.133	1
Gaussian mode purity	98%	99.8% (100% desired)
Astigmatism $\Delta z_0(mm)$	60.5	3.25 (0 desired)

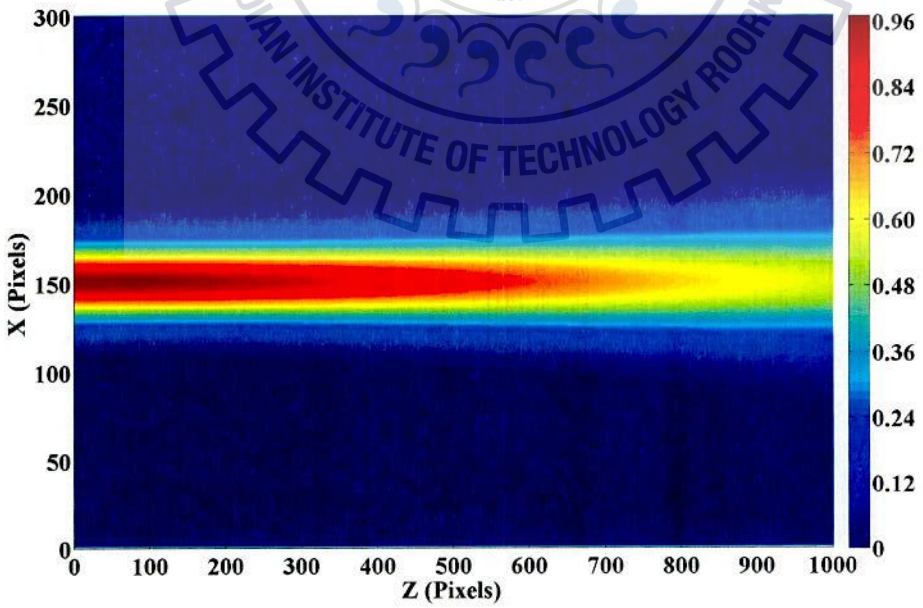

Figure 4.7: Side view of propagating wave.

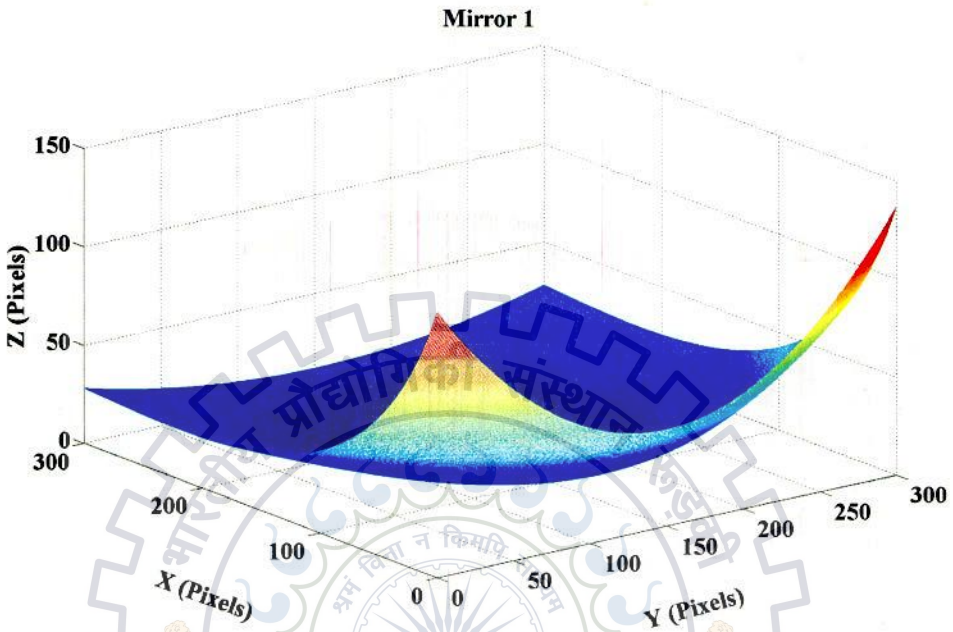

Figure 4.8: Mirror 1 profile.

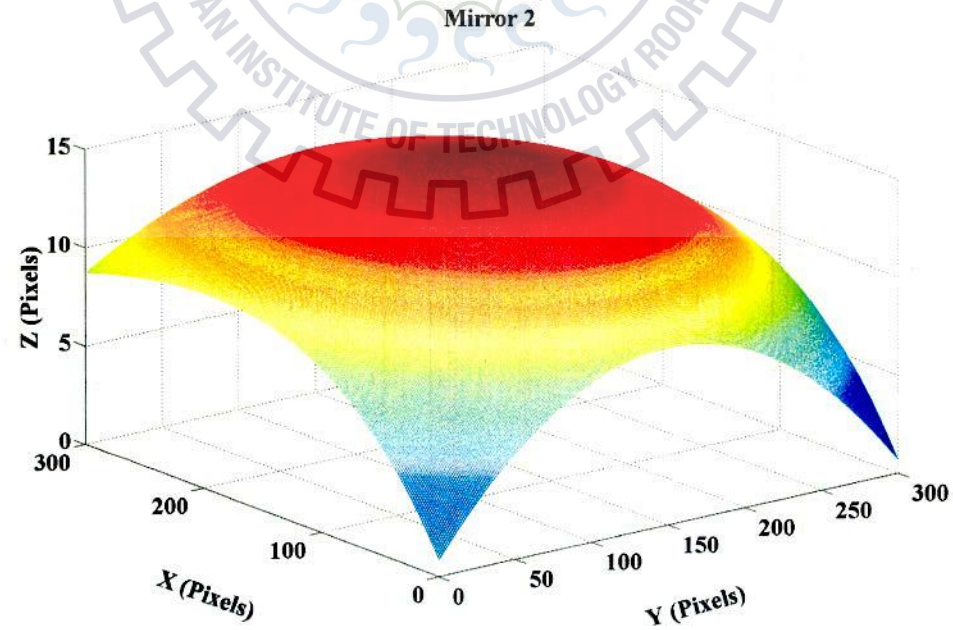

Figure 4.9: Mirror 2 profile.

Chapter 5

Conclusion And Future Scope

5.1 Conclusion

The work presented in the previous chapters is a conceptual design of 170 GHz, MW class, CW gyrotron for ECRH applications in the thermonuclear fusion reactors for ITER or ITER- like projects. By the Self-C calculations we achieved the efficiency around 37 % and delivering power is around the 1.1-1.3 MW. The required magnetic field is achieved by settling the no. of turns of the coils and by varying current and voltage in the coils.

The first step of designing of this gyrotron is mode selection. After following the mode selection procedure the selected mode is $TE_{28,12}$. To achieve minimum reflection, the gyrotron's cold cavity is designed using the self consistent calculations. Multi-mode time dependent calculations are also done. A magnetic guidance system and a diode type magnetron injection gun is designed using the ESRAY code. The achieved magnetic field at the center of the cavity is 6.725 T. The output system is designed which includes a non - linear taper with 99.50 % of transmission, a quasi - optical launcher which gives 99.68 % Gaussian mode content and RF-window. The latest update is done in GDS V3 with phase retrieval methods (Iterative and Irradiance) and Mirror Synthesis. Using this update a two mirror MOU is designed.

5.2 Future Scope

This research work can be extended into following tasks:

- The design study for this gyrotron has been done for the fundamental harmonic. This can also be designed for the further harmonics with improved structure. The higher harmonic operation require less magnetic field at the interaction but the efficiency decreases.

- The same gyrotron can be built using the coaxial cavity to improve the efficiency so that the output power can be achieved more.

- The Self-T calculations will be calculate to explore the multi-mode behavior of this gyrotron. The Self-T analysis will give the information that the gyrotron is capable to give power continuously or not. This analysis performed the CW operation of gyrotron.

- Using the single stage depressed collector the efficiency can be improved from 37 % to more than 50 %.

- The iterative phase retrieval method is used to reconstruct the phase. Merging it with irradiance moment method a new approach can be developed with the name as "Iterative irradiance method". The new proposed method can reconstruct the phase with better efficiency.

- The two mirror system MOU is designed for this gyrotron. Using the same approach presented in chapter 4 an internal mode converter unit can also be designed.

Bibliography

[1] M. V. Kartikeyan, E. Borie, and M. K. A. Thumm, "Gyrotrons- High Power Microwave and Millimeter Wave Technology," *Berlin, Germany: Springer*,2004.

[2] Kuntze, M., Alberti, S., Dammertz, G., Giguet, E., Illy, S., Heidinger, R., Koppenburg, K., LeCloarec, G., Legoff, Y., Leonhardt, W., Piosczyk, B., Schmid, M., Thumm, M.K., Tran, M.Q., "Advanced high-power gyrotrons," *IEEE Transactions on Plasma Science*,vol. 31, no. 1, pp. 25 - 31, Feb 2003.

[3] M. Thumm, "State-of-the-Art of High Power Gyro-Devices and Free Electron Masers Update 2013," *Karlsruhe Institute of Technol-ogy KIT scientific report 7641, Germany*, 2014.

[4] T. Rzesnicki, B. Piosczyk, S. Kern, S. Illy, J. Jin, A. Samartsev, A. Schlaich, M. Thumm, "2.2-MW Record Power of the 170-GHz European Preprototype Coaxial-Cavity Gyrotron for ITER," *IEEE Transactions on Plasma Science*,vol.38, no.6, pp.1141-1149, June 2010.

[5] S. Pradhan, A.N. Sharma, V.L. Tanna, Z. Khan, U. Prasad, K. Doshi, D.C. Raval, F. Khan, N.C. Gupta, J. Tank,"SST-1 Status and Plans," *IEEE Transactions on Plasma Science*, vol.40, no.3, pp.614-621, March 2012.

[6] Kwo Ray Chu "Overview of research on the gyrotron traveling-wave amplifier," *IEEE Trans. Plasma Sci.*, vol.30, no.3, pp. 903-908, Jun 2002.

[7] A. V. Gaponov-Grekhov and V. L. Granatstein, "Application of High-Power Mi-crowaves," *Boston, MA: Artech House* , 1994.

[8] M. Thumm "Recent applications of millimeter and submillimeter wave gyrotrons," *infrared and Millimeter Waves 2000* , 2000.

[9] M. Thumm "Novel applications of millimeter and submillimeter wave gyro-devices," *Int. J. Infrared Millim. Waves* , vol. 22, pp. 377-386, 2001.

[10] Manfred Thumm "Progress on Gyrotrons for ITER and Future Thermonuclear Fusion Reactors," *IEEE Trans. Plasma Sci.*, vol.39, no.4, pp. 971-979, April 2011.

[11] K. Sakamoto, K. Kajiwara, Y. Oda, K. Takahashi, K. Hayashi, N. Kobayashi, "Development of high power long pulse gyrotron in JAEA," *36th International Conference on Infrared, Millimeter and Terahertz Waves (IRMMW-THz))*, pp.1-3, Oct. 2011.

[12] K. Sakamoto, A. Kasugai, K. Takahashi, R. Minami, N. Kobayashi, K. Kajiwara, "First experimental results from the European Union 2-MW coaxial cavity ITER gyrotron prototype ," *Nature Physics*,Vol. 3, pp. 411-414, 2008.

[13] K. Sakamoto,A. Kasugai, K. Takahashi, R. Minami, N. Kobayashi, K. Kajiwara, Y. Oda, K. Hayashi, "Progress of high power 170 GHz gyrotron in JAEA," *Nucl. Fusion*, Vol. 49, 2009.

[14] K. Sakamoto, K. Kajiwara, Y. Oda, K. Takahashi, K. Hayashi, N. Kobayashi, "Long pulse and high power repetitive operation of the 170 GHz ITER gyrotron," *J. Plasma and Fusion Research, letters*, Vol. 4, pp. 006-1 006-3, 2009.

[15] Y. Oda, M. Ushio, K. Komurasaki, K. Takahashi, A. Kasugai, K. Sakamoto, "Application of high power millimeter-wave to space propulsion," *The Joint 30th International Conference on Infrared and Millimeter Waves and 13th*

International Conference on Terahertz Electronics (IRMMW-THz)), pp.30-31, 19-23 Sept. 2005.

[16] A. Kasugai, R. Minami, K. Takahashi, N. Kobayashi, K. Sakamoto, "Development of a 170GHz high-power and CW gyrotron for fusion application," *The Joint 30th International Conference on Infrared and Millimeter Waves and 13th International Conference on Terahertz Electronics (IRMMW-THz))*, pp.287-288, 19-23 Sept. 2005.

[17] A. Kasugai, K. Takahashi, N. Kobayashi, K. Sakamoto, "Development of 170GHz Gyrotron for ITER," *The Joint 31st International Conference on Infrared and Millimeter Waves and 14th International Conference on Terahertz Electronics (IRMMW-THz))*, pp.202, 18-22 Sept. 2006.

[18] K. Sakamoto, "Gyrotrons and mm wave technology for ITER," *The Joint 32nd International Conference on Infrared and Millimeter Waves and 15th International Conference on Terahertz Electronics (IRMMW-THz))*, pp.4-7, 2-9 Sept. 2007.

[19] K. Sakamoto, A. kasugai, K. Kajiwara, K. Takahashi, N. Kobayashi, "Demonstration of high efficiency 1MW oscillation by 170GHz CW Gyrotron," *The Joint 32nd International Conference on Infrared and Millimeter Waves and 15th International Conference on Terahertz Electronics (IRMMW-THz))*, pp.708-709, 2-9 Sept. 2007.

[20] K. Sakamoto,A. Kasugai, K. Takahashi, K. Kajiwara, Y. Oda, "Reliability test of the ITER 170 GHz gyrotron and development of the two-frequency gyrotron," *IEEE Int. Vacuum Electronics Conference (IVEC 2010)* , Monterey, USA, pp. 31-32, 2010.

[21] M.V. Agapova, G.G. Denisov, V.I. Kurvatov, A.G. Livak, V.E. Myasnikov, V.O. Nichiporenko, L.G. Popov, E.A. Soluyanova, E.M. Tai, S.V. Usachev, V.E. Zapevalov, "Development of 1 MW output power level gyrotrons for

fusion systems," *Abstracts International Vacuum Electronics Conference*, Monterey, CA, USA, 02-04 May 2000.

[22] V.E. Zapevalov, V.A. Flyagin, A.N. Kuftin, V.K. Lygin, "Electron beam-cavity system of 170 GHz gyrotron for ITER," *25th International Conference on Infrared and Millimeter Waves*, Beijing, China, pp. 25 - 26, 12-15 Sept. 2000.

[23] V.E. Myasnikov, A.G. Litvak, S.V. Usachev, L.G. Popov, "Development of 170 GHz gyrotron for ITER," *Third IEEE International Vacuum Electronics Conference*, pp. 334 - 335, 2002.

[24] M.V. Agapova, G.G. Denisov, V.I. Ilyin, A.G. Litvak, V.E. Myasnikov, L.G. Popov, S.V. Usachev, V.E. Zapevalov, E.M. Tai, "Recent Results in the Development of 170 GHz/CW Gyrotrons for ITER ," 31^{st} *Int. Conf. on Infrared and Millimeter Waves*, Shanghai, China, pp. 516 - 518, 2006.

[25] A.G. Litvak, V.E. Myasnikov, S.V. Usachev, L.G. Popov, M.V. Agapova, V.O. Nichiporenko, G.G. Denisov, A.A. Bogdashov, A.Ph. Gnedenkov, V.I.Ilyin, V.N. Ilyin, D.V. Khmara, A.N. Kostyna, A.N. Kuftin, V.K. Lygin, M.A. Moiseev, V.I. Malygin, E.A. Salujanova, V.E. Zapevalov, E.M. tai, "Development of 170 GHz/1 MW/ 50% CW gyrotron for ITER," 29^{th} *Joint 29th International Conference on Infrared and Millimeter Waves and 12th International Conference on Terahertz Electronics*, pp. 111 - 112, 27 Sept.-1 Oct. 2004.

[26] A.G. Litvak, G.G. Denisov, M.V. Agapova, A.P. Gnedenkov, A.N. Kostyna, V.O. Nichiporenko, V.E. Myasnikov, L.G. Popov, E.M. tai, S.V. Usachev, V.E. Zapevalov, A.V. Chirkov, V.I. Ilin, V.N. Ilin, A.N. Kuftin, S.A. Malygin, V.I. Malygin, V.V. Parshin, A.B. Pavel'ev, V.G. Rukavishnikova, Yu.V. Roschin, E.V. Sokolov, E.A. Soluyanova, A.L. Vikharev, "Development in Russia of 170 GHz gyrotron for ITER," 29^{th} *IEEE International Vacuum Electronics Conference*, Rome, pp. 281 - 282, 28-30 April 2009.

[27] A.G. Litvak, G.G. Denisov, M.V. Agapova, V.E. Myasnikov, L.G. Popov, E.M. tai, S.V. Usachev, V.E. Zapevalov, A.V. Chirkov, V.I. Ilin, V.N. Ilin, A.N. Kuftin, V.I. Malygin, E.V. Sokolov, E.A. Soluyanova, "Development in Russia of 170 GHz gyrotron for ITER," 36^{th} *International Conference on Infrared, Millimeter and Terahertz Waves (IRMMW-THz)*, Houston, TX, pp. 1 - 3, 2-7 Oct. 2011.

[28] M.V. Agapova, G.G. Denisov, V.I. Ilyin, V.N. Kostyna, A.G. Litvak, V.E. Myasnikov, L.G. Popov, S.V. Usachev, V.E. Zapevalov, E.M. Tai,*New test results of 170 GHz/1 MW/50% /CW gyrotron for ITER*, 32^{nd} *Int. Conf. on Infrared and Millimeter Waves* , Cardiff, UK, pp. 44-45, 2007.

[29] B. Piosczyk, O. Braz, G. Dammertz, C.T. Iatrou, S. Illy, M. Kuntze, G. Michel, M. Thumm, "165 GHz, 1.5 MW-Coaxial cavity gyrotron with depressed collector," *IEEE Trans. on Plasma Science*, vol. 27, pp. 484–489, 1999.

[30] B. Piosczyk, A. Arnold, O.S. Lamba, O. Braz, G. Dammertz, C.T. Iatrou, M. Kuntze, G. Michel, M. Thumm, "Step-frequency operation of a coaxial cavity from 134 to 169.5 GHz," *IEEE Trans. on Plasma Science*, vol. 28, pp. 918–923, 2000.

[31] M.V. Kartikeyan, E. Borie and M.K. Thumm, "Possible Operation of a 1.5-2 MW, CW Conventional Cavity Gyrotron at 140 GHz," *IEEE Trans. on Plasma Science*, vol. 28, no. 3, pp. 645–651, June 2000.

[32] G. Dammertz et. al. "1 MW, 140 GHz, CW Gyrotron for Wendelstein 7-X," *25th International Conference on Infrared and Millimeter Waves*, Beijing, China, pp. 15 - 16, 12-15 Sept. 2000.

[33] G. Dammertz, O. Braz, A. K. Chopra, K. Koppenburg, M. Kuntze, B. Piosczyk, and M. Thumm, "Recent Results of the 1-MW, 140-GHz, $TE_{22,6}$-Mode Gyrotron," *IEEE Trans. on Plasma Science*, vol. 27, no. 2, pp. 330 - 339, April 1999.

[34] M. Thumm et. al., "Progress in the 10-MW 140-GHz ECH System for the Stellarator W7-X," *IEEE Trans. on Plasma Science*, vol. 36, no. 2, pp. 341 - 355, April 2008.

[35] B. Piosczyk, G. Dammertz, O. Dumbrajs, M.V. Kartikeyan, M.K. Thumm and X. Yang "165-GHz Coaxial Cavity Gyrotron," *IEEE Trans. on Plasma Science*, vol. 32, no. 3, pp. 853–860, June 2004.

[36] X. Yang, B. Piosczyk, D. Wagner, E. Borie, R. Heidinger, G. Dammertz and M. Thumm, "Analysis of transmission characteristics for single and double disk windows," *Twenty Seventh International Conference on Infrared and Millimeter Waves*, San Diego, CA, USA, pp. 157 - 158, 26-26 Sept. 2002.

[37] N. C. Chauhan, M. V. Kartikeyan and A. Mittal "CAD of RF Windows Using Multiobjective Particle Swarm Optimization," *IEEE Trans. on Plasma Science*, vol. 37, no. 6, pp. 1104–1109, June 2009.

[38] M. Airila, *Electron Energy Spectra in Gyrotrons with Depressed Collectors*, Master's thesis, Helsinki University of Technology, Department of engineering physics and mathematics, November 2000.

[39] K. L. Felch, B. G. Danly, H. R. Jory, K. E. Kreischer, W. Lawson, B. Levush, R.J. Temkin, "Characteristics and applications of fast-wave gyrodevices," *Proceedings Of The IEEE*, vol. 87, no. 5, pp. 752-781, May 1999.

[40] R.A. Olstad, J.L. Doane, C.P. Moeller, R.C. O'Neill, M. DiMartino, "High-power corrugated waveguide components for mm-wave fusion heating systems," in *19th Symposium on Fusion Technology*, Lisbon, Portugal, 16-20 Sep. 1996.

[41] A. V. Gaponov, V. A. Flyagin, A. L. Goldenberg, G. S. Nusinovich, S.E. Tsimring, V. G. Usov, and S. N. Vlasov, "Powerful millimeter-wave gyrotrons," *International Journal of Electronics* , vol. 51, pp. 277, 1981.

[42] S. N. Vlasov, G. M. Zhislin, I. M. Orlova, M. I. Petelin, G. G. Rogacheva, "Irregular waveguides as open resonators," *Radiophysics Quantum Electronics*, vol. 12, pp. 972-978, 1969.

[43] M.V. Kartikeyan, E. Borie, B. Piosczyk, O. S. Lamba, V. V. P. Singh, A. Mobius, H. N. Bandopadhyay, and M. Thumm, "Conceptual design of a 42 GHz, 200 kW gyrotron operating in the $TE_{5,2}$ mode," *International Journal of Electronics*, vol. 87, pp. 709–723, 2000.

[44] G.G. Denisov, V.E. Zapevalov, A.G. Litvak, and V.E. Myasnikov, "Megawatt gyrotrons for cer heating and current-drive systems in controlled-fusion facilities," *Radiophysics and Quantum Electronics*, vol. 46, no. 10, pp. 757-768, 2003.

[45] W. G. Lawson, "Theoretical evaluation of non-linear tapers for a high power gyrotrons," *IEEE Transactions on Microwave Theory and Techniques*, vol. 38, no. 11, pp. 1617-1622, 1990.

[46] J. Jin, B. Piosczyk, M. Thumm, T. Rzesnicki, and S. Zhang, "Quasi-optical mode converter/mirror system for a high power coaxial-cavity gyrotron," *IEEE Transactions on Plasma Science*, vol. 34, no. 4, pp. 1508-1515, Aug. 2006.

[47] Y. Hirata, Y. Mitsunaka, K. Hayashi, Y. Itoh, K. Sakamoto and T. Imai , "The Design of a Tapered Dimple-Type Mode Converter/Launcher for High-Power Gyrotrons," *IEEE Transactions on Plasma Science*, vol. 3, no. 1, pp. 142-145, 2003.

[48] M. Thumm, "Quasi-optical gyrotron mode converters," in *Colloquium on Gyrotrons, 6th Greek School on Fusion Physics and Technology*, University of Thessaly, Volos, Greece, 26–31 March 2007.

[49] T.V. George, "High average power microwave sources for fusion research," in *International Vacuum Electronics Conference*, Abstracts, pp. 1-2(18.1), May 2000.

[50] Ragini Jain and M. V. Kartikeyan, "Design Studies of a 100 kW, 60 GHz CW Gyrotron for Plasma Diagnostics," *Progress In Electromagnetics Research B*, Vol. 22, 379-399, 2010.

[51] Stefan Illy, "*ESRAY– A computer code for the analysis of axisymmetric electron guns*," Private communication, 2002.

[52] J. M. Baird and W. Lawson, "Magnetron Injection Gun (MIG) Design for Gyrotron Applications," *Int. Journal Electronics*, Vol. 61, Pg. 969-984, 1986.

[53] M.V. Kartikeyan, E. Borie, B. Piosczyk, O. S. Lamba, V. V. P. Singh, A. Mobius, H. N. Bandopadhyay, and M. Thumm, "Conceptual design of a 42 GHz, 200 kW gyrotron operating in the $TE_{5,2}$ mode," *Int. Journal Electronics*, vol. 87, pp. 709-723, 2000.

[54] J. R. Fienup, "Phase retrieval algorithms : A comparison ," *Applied Optics.*, vol. 21, issue 15, pp. 2758-2769, 1982.

[55] D. R. Denison, T. S. Chu, M. A. Shapiro, and R. J. Temkin, "Gyrotron Internal Mode Converter Reflector Shaping from Measured Field Intensity," *IEEE Transactions on Plasma Science*, Vol. 27, No. 2, pp. 512-519, Apr. 1999 .

[56] A. A. Bogdashov, G.G.Denisov "Synthesis of the Sequence of Phase Correctors Forming the Desired Field," *Radiophysics and Quantum Electronics*, Vol. 47, No. 12, 2004.

[57] R. W. Gerchberg, W. O. Saxton "A Practical Algorithm for the Determination of Phase from Image and Diffraction Plane Pictures," *Optik*, Vol. 35, pp. 237-246, 1972 .

[58] Jawla, S., Hogge, J.P., Alberti, S., "Theoretical Investigation of Iterative Phase Retrieval Algorithm for Quasi-Optical Millimeter-Wave RF Beams," *IEEE Trans. Plasma Sci.*, vol.37, Issue.3, pp.403-413, March 2009.

[59] Jawla, S.K., Hogge, J.-P. ; Alberti, S., "Analysis of iterative phase retrieval approach to optimize amplitude measurement parameters," *Infrared and Millimeter Waves, 15th International Conference on Terahertz*, 2-9 Sept. 2007.

[60] Jianbo Jin, Gerd Gantenbein, John Jelonnek, Manfred Thumm and Tomasz Rzesnicki, "A New Method for Synthesis of Beam-Shaping Mirrors for Off-Axis Incident Gaussian Beams," *IEEE Trans. Plasma Sci.*, 2014.

List of Publications

Journal publications

- **Ravi Kumar Dhakad**, Gaurav S. Baghel, M.V. Kartikeyan and Manfred K. Thumm,"Output system for a 170 GHz/1.5 MW Continuous Wave Gyrotron Operating at the $TE_{28,12}$ Mode," *IEEE Trans. on Plasma Science* [communicated]

Conference publications

- **Ravi Kumar Dhakad**, Sukwinder Singh, G.S. Baghel, J. Malik, M.V. Kartikeyan, "Iterative Phase Retrieval Algorithm for Gyrotron," *National conference on Vacuum Electronic Devices & Applications, VEDA KOLLEG-2013,* Oct. 18-20,2013, IIT Roorkee, India.